ZANKO GROUNDWATER POTENTIAL EVALUATION OF U/MAI USING ELECTRICAL RESISTIVITY METHOD

BY

ADEPOJU SHERIF OYEWOLE

NSU/PGD/GEP/0003/17/18

PROJECT SUBMITTED TO THE SCHOOL OF POSTGRADUATE STUDIES, NASARAWA STATE UNIVERSITY KEFFI, IN PARTIAL FULFILLMENT OF THE REQUIREMENT FOR THE AWARD OF DEGREE OF PGD IN PHYSICS

DEPARTMENT OF PHYSICS

FACULTY OF APPLIED AND NATURAL SCIENCE, NASARAWA STATE UNIVERSITY, KEFFI,

NIGERIA.

SEPTEMBER, 2018

DECLARATION

I hereby declare that this Project has been written by me and it is a report of my Field work/research. It has not been presented in any previous application for Post Graduate Diploma Degree. All quotations are indicated and sources of information specifically acknowledged means references

_____

ADEPOJU SHERIF OYEWOLE

NSU/PGD/GEP/0003/l7/18

CERTIFICATION

The project titled "Groundwater Potential Evaluation of U/Mai Zanko Using Electrical Resistivity Method" meets the regulations governing the award of Post Graduate Degree, of the School of Post-graduate studies, Nassarawa State University, Keffi and is approved for its contribution to knowledge.

ACKNOWLEDGEMENTS

I feel obliged to acknowledge those who stood by me in the course of this Programme. First and foremost, all honor and adoration be unto God Almighty for being merciful, faithful and gracious unto me and my entire family members.

I would like to place on permanent record the efforts and kindness of Prof. Charles Ofiodile who has been of encouragement to me. My profound gratitude goes to my supervisor, Dr. Olatunji S. Ayanninuola Who closely worked with me during the period of this study. I also wish to express my profound gratitude and appreciation to the lectures, staff of the department for their advice, criticisms and suggestions in improving the quality of this work.

I would like to express my gratitude to the Head of Department, Prof. Umar Gurku, My horizon in the geologic field has been broadened and as such I want I want to extent my warmest regards to you all.

With utmost sincerity, I like to say a big thanks to my wife and Children for their prayers, patience and love. I am very grateful to for their enormous assistance, encouragement and kindness.

To all my Bosses and colleagues, especially Mr. Abbey. I am very grateful.

TABLE OF CONTENT

Cove page - - -

Title page - - - - - - i

Declaration - - - - - ii

Certification - - - - - iii

Acknowledgement - - - - iv

Table of content - - - - - v

List of Table - - - - - - - - - - viii

List of Plate - - - - - - - - - ix

List of Figure - - - - - x

Abstract- - - - - xii

CHAPTER ONE

INTRODUCTION

1.1 Background to the study - - - - 1

1.1.1 Origin of Groundwater - - - - 4

1.1.2 Groundwater and Hydrologic Cycle - - - 4

1.1.3 The Occurrence of Subsurface Water - - 9

1.1.4 Transmission of Groundwater- - - - - 11

1.1.5 Recharge - - - - - - - 11

1.1.6 Leakage - - - - - 12

1.1.7 Aquifers - - - - - 12

1.3 Statement of the Problem - - - 15

1.4 Aim and Objectives - - - - 15

CHAPTER FOUR

RESULTS ANI) 1)ISCUSSION

4.1 Field curves - - - - - - - - 40

4.2 Top layer resistivity - - - - - - - - 46

4.3 Overburden thickness (depth to basement) - - - - - 46

4.4 True aquifer resistivity - - - - - - - - 48

4.5 True aquiferthickness - - - - - - - - 48

4.6 Groundwater potential zone - - - - - - - 48

CHAPTER FIVE

SUMMARY, CONCLUSION AND RECOMMENDATION

5.1 Summary - - - - - - - - - - 51

5.2 Conclusion - - - - - 51

2.3 Recommendations - - - - 52

REFERENCES - - - - 53

APPENDICES - - - - 54

LIST OF TABLE

Table 4.1 Summary of VES result across the study area - - - 41

Table 4.2 Characteristic curve types in the area with their frequency and percentage 42

LIST OF PLATE

Plate 1: PASI 16GL (Resistivity Meter) and its Accessories - - - - 36

LIST OF FIGURE

Figure 1.1: The Hydrological Cycle (Kevin, 2005) - - - - - 6

Figure 1.2: The distribution of water at or near the Earth's surface (Kevin, 2005) - 8

Figure 1.3: A schematic cross-section showing the typical distribution of subsurface waters in a simple 'unconfined" aquifer setting, highlighting the three common subdivisions of the unsaturated zone and the saturated zone below the water table (Kevin, 2005) - 10

Figure 1.4: Hydrological cycle and aquifers type (Harlan et al., 1989) - - 14

Figure 2.1: The Schiumberger array configuration (Telford et al., 1990) - 23

Figure 2.2: General four electrode array (Telford ci al., 1990) - - - 23

Figure 2.3: A conventional four electrode array to measure the subsurface resistivity 29

Figure 2.4: Common arrays used in resistivity surveys and their geometric factors (Loke, 1997, 1999)- - - - - - - - - - - 30

Figure 2.5: Dipole -Dipole Array Configuration (Loke, 1999)

Figure 2.6: Dipole-Dipole Array Configuration (Milsom, 1996)

Figure 2.7: The forward and reverse pole-dipole arrays -

Figure 3.1: Location Map of the Area - - -

Figure 3.2: Drainage Map of the Area - - -

Figure3.3: Geological Map of the Area - - -

Figure3.4: Geological Map with VES Points - -

Figure 4.1 Typical H-type curve in the study area - -

Figure 4.2 Typical HA-type curve in the study area - -

Figure 4.3 Typical Q1-l-type curve in the study area -

Figure 4.4 Typical KH-type curve in the study area -

Figure 4.5 Typical QHA-type curve in the study area -

Figure 4.6 Typical KQH-type curve in the study area - - - - 45

Figure 4.7 Top layer resistivity map - - - - - 47

Figure 4.8 Overburden thickness map - - - - 47

Figure 4.9 True aquifer resistivity map - - - - 49

Figure 4.10 True aquifer thickness map - - - - 49

Figure 4.11 Map of groundwater potential zones - - - 50

ABSTRACT

Groundwater represents the most reliable source of potable water especially in the rural area where treated water from municipal water supply is virtually non-existent and the people rely on water from surface sources and shallow wells for their drinking and other domestic uses. These are relatively unsafe and pose health risks. For this reason, 30 schlumberger VES were conducted along gridded profile across Ungwan Mai Zanko and environs bounded by latitude N9.00 - N9.04 and longitudes E8.24 - E8.29 within the Basement Complex of Central Nigeria, using Omega resistivity metre made by Allied company and its accessories to evaluate the groundwater potential of the area. The VES result interpretation using IPJ2win soft program reveal a maximum of five (5) geoelectric layers with six (6) different curve types in the subsurface within the study area. The geoelectric parametres obtained from the VES interpretation were used to categorise the area into three (3) groundwater potential zones based on the resistivity and thicknesses of the true aquifer and the overburden thickness (depth to basement). The study reveal the area to be of generally good groundwater potential, with the central portion particularly promising for groundwater based on the low resistivity and high aquifer thickness as well as high overburden thickness found in the area.

CHAPTER ONE

INTRODUCTION

1.1 Background to the study

Access to clean water is a human right and a basic requirement for economic development. The safest kind of water supply is the use of groundwater. Since groundwater normally has a natural protection against pollution by the covering layers, only minor water treatment is required. Detailed knowledge on the extent, hydraulic properties, and vulnerability of groundwater reservoirs is necessary to enable a sustainable use of their sources (Kirsch, 2006).

Groundwater is the water held in the subsurface within the zone of saturation under hydrostatic pressure below water table (Ariyo & Banjo, 200$). Groundwater is commonly understood to mean water occupying all the voids within a geologic stratum (Todd & Mays, 2005).

Groundwater and other mineral resources such as hydrocarbons and solid minerals are of great abundance in Nigeria. Potable water is one of the major resources that a citizen of any nation can benefit from (Alile & Amadasun, 2008). This is so because water is a free course of nature. It is a gift of God to mankind. This wonderful resources have transcended so many generations because of its value to human life. Water is one of the major determinants of economic development. It has found, its' usefulness in every human endeavor such as manufacturing industry, agricultural industry, transportation industry, construction industry, home usage and so on (Alile & Amadasun, 2008).

At present, groundwater via shallow hand dug wells and few borehole constructions constitutes a major source of drinking water supply in Aclakomu, village. The yields are somewhat variable and less than expected average considered enough for the overall populace. In order to ease the problem of water scarcity and improve the living standard of the comm unity this study was embarked upon to delineate the subsurface geological sequences and their hydrogeological characteristics/groundwater potentials in the light of the notably sustainable groundwater yield of typical basement terrains. Generally, surface water accumulates after precipitation under the influence of gravity in rock cavities as a vast groundwater reservoir supplying wells, boreholes, springs and flowing streams (Flarr, 1962). In a typic& Precambrian Basement Complex area, this

groundwater reservoir is usually contained within the weathered and the tectonically induced geological features; fractured/fissured, sheared or jointed/faulted basement columns of the rock unit(s). These geological processes alter the rock units to reduce resistivity at depth of burial and hence increase the porosity and permeability of such units for groundwater accumulation, discharge and exploitation. This, therefore, constitutes the basis of the choice of electrical resistivity survey method in this present study.

The urban and rural residents in several parts of Nigeria are battling with inadequate availability of potable water for domestic and industrial usage. This difficulty is on daily increase due to the continuous increase in population and industrialization across the country. As a consequence, the demand for clean water is on the increase and the available surface water cannot be depended on because they have been highly polluted and also the supply is inadequate. In addition to being vulnerable to pollution, surface water sources are also easily affected by extreme weather conditions consequent upon which they are considered as unreliable, unsuitable and unsustainable in many parts of the world (Adiat et aL, 2012).

The Basement Complex of Africa is a heterogeneous mixture of crystalline rocks predominantly of granitic or gneissose character. Groundwater occurs within these crystalline rocks in fissures or in the superficial weathered zones. The rocks are relatively impermeable and groundwater can occur in the superficial deposits overlying the bedrock. There are no regional aquifers in Basement complex country and each site has to be treated as unique (Clark, 1985)

The basis of any geophysical method is measuring a contrast between physical properties of the target and the environs. The better the contrast or anomaly, the better the geophysical response and hence the identification. So, the efficiency of any geophysical technique lies in its ability to sense and resolve the hidden subsurface hydrogeological heterogeneities or variation. Hence for groundwater exploration, a judicious application or integration of techniques is most essential for success in exploration, technologically as well as economically (Rosli et al., 2012).

Therefore, the application of geophysics to the successful exploration of groundwater in sedimentary terrain requires a proper understanding of its hydro-geological characteristic. Evidence has shown that geophysical methods are the most reliable and the most accurate means

of all surveying method of subsurface structural investigations and rock variation (Carruthers, 1985; Emenike, 2001).

Due to the successful application of electrical resistivity over the years in groundwater exploration, this propels me to adopt electrical resistivity method to investigate groundwater potential and geological structure of the study area. However, electrical resistivity surveys have undergone significant changes in the last three decades. The traditional horizontal layering technique for investigating electrical resistivity data are rapidly being replaced with 2-dimensional and 3- dimensional models of interpretation especially in complex and heterogeneous subsurface media (Aizebeokhai, 2010).

Field techniques have advanced frOm manual measurements made at separate and independent points to the use of automated machine with multi-electrode array along the measurement profile. Till 1980s, data acquisition was more or less carried out manually and this is demanding and slow and the quality of the measured data is poor. Therefore, a range of fast automated multi-electrode and multichannel data acquisition system now exists that follows flexibility in the acquisition of electrical resistivity data (Barker, 1981; Stummer and Maurer, 2001; Auken et al., 2006).

For the purpose of this study, the application of electrical resistivity methods using 2D electrical resistivity via the Wenner array and Vertical Electrical Sounding (VES) via the Schiumberger array were employed in order to delineate the Aquifer unitsat Adakomu village, Ewuji community in Abeokuta, Southwestern Nigeria.

1.1.1 Origin of Groundwater

The origin of groundwater is primarily one of the following — Groundwater derived from rainfall and infiltration within the normal hydrological cycle, this kind of water is called meteoric water. The name implies recent contact with the atmosphere; Groundwater encountered at great depths in sedimentary rocks as a result of water having been trapped in marine sediments at the time of their deposition, this type of groundwater is referred to as connate waters. These waters are normally saline. It is accepted that connate water is derived mainly or entirely from entrapped sea water as original sea water has moved from its original place. Some trapped water may be brackish; Fossil water if fresh may be originated from the fact of climate change phenomenon,

i.e., some areas used to have wet weather and the aquifers of that area were recharged and then the weather of that area becomes dry.

1.1.2 Groundwater and Hydrologic Cycle

The hydrological cycle, as depicted in Fig. 2.1, can be thought of as the continuous circulation of water near the surface of the Earth from the ocean to the atmosphere and then via precipitation, surface runoff and groundwater flow back to the ocean. Warming of the ocean by solar radiation causes water to be evaporated into the atmosphere and transported by winds to the landmasses where the vapor condenses and falls as precipitation. The precipitation is either returned directly to the ocean, intercepted by vegetated surfaces and returned to the atmosphere by evapotranspiration, collected to form surface runoff, or infiltrated into the soil and underlying rocks to form groundwater. The surface runoff and groundwater flow contribute to surface streams and rivers that flow to the ocean, with pools and lakes providing temporary surface storage (Kevin, 2005).

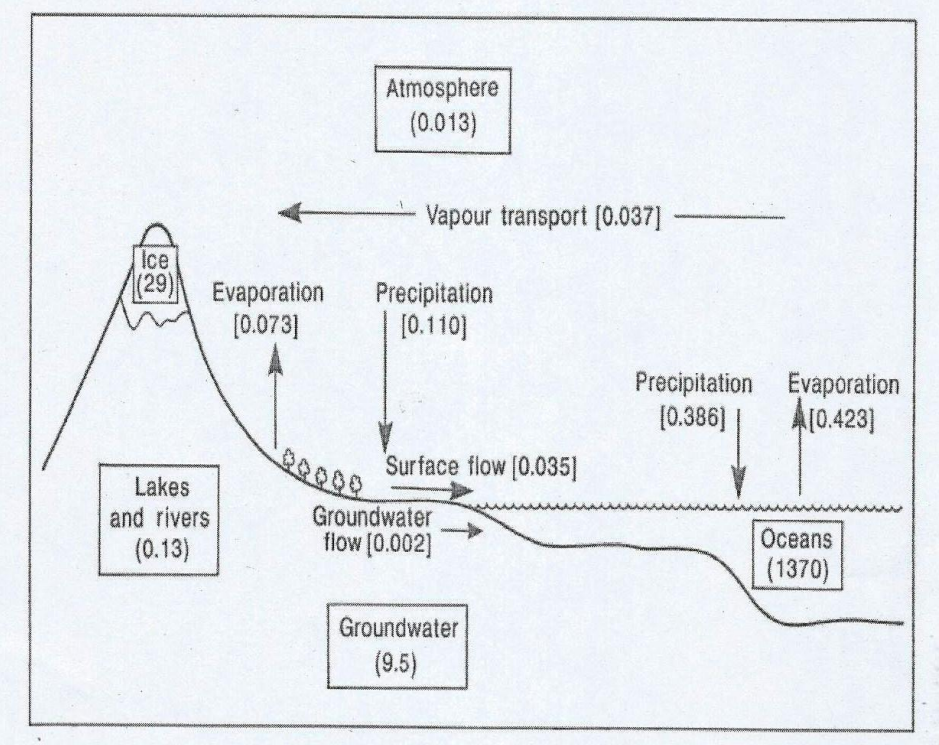


Figure 1.1: The Hydrological Cycle (Kevin, 2005).

Of the total water in the global cycle, Fig. 2.1 shows that saline water in the oceans accounts for97.25% (Kevin, 2005). Land masses and the atmosphere therefore contain 2.75%. Ice caps and glaciers hold 2.05%, groundwater to a depth of 4 km accounts for 0.68%, freshwater lakes 0.01%, soil moisture 0.005% and rivers 0.0001% (Kevin, 2005). About 75% of the water in land areas is locked in glacial ice or is saline. The relative importance of groundwater can be realized when it is considered that, of the remaining quarter of water in land areas, around 98% is stored underground. In addition to the more accessible groundwatcr involved in the water cycle above a depth of 4 km, estimates of the volume of interstitial water in rock pores at even greater depths range from 53 x 106 km3 (Ambroggi, 1977) to 320 x 106 km3 (Garrels etal., 1975).

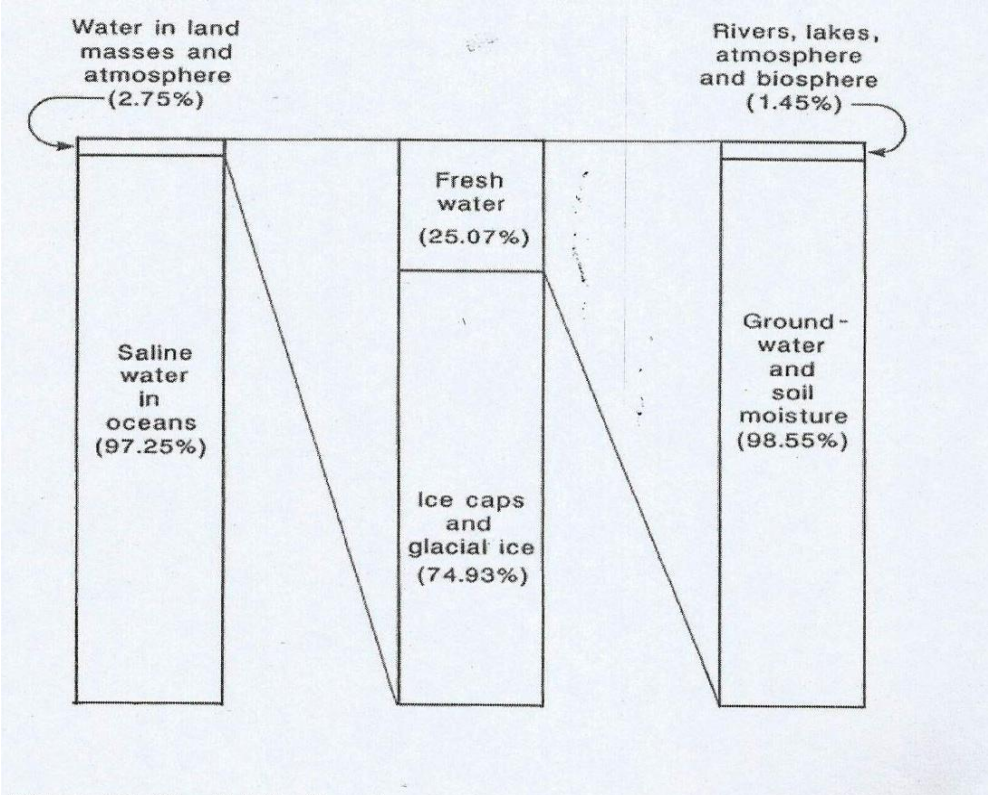


Figure 1.2: The distribution of water at or near the Earth's surface (Kevin, 2005)

1.1.3 The Occurrence of Subsurface Water

The subsurface occurrence of groundwater may be divided into zones of aeration and saturation. The zone of aeration consists of interstices occupied partially by water and partially by air. In the zone of saturation all interstices are filled with water, under hydrostatic pressure. One most of the landmasses of the earth, a single zone of aeration overlies a single zone of saturation and extends upward to the ground surface, as shown in Figure 2.3. In the zone of aeration (unsaturated zone), Vadose water occurs. This general zone may be further subdivided into the soil water zone, the intermediate Vadose zone (sub-soil zone), and capillary zone (Figure 2.3). The saturated zone extends from the upper surface of saturation down to underlying impermeable rock In the absence of overlying impermeable strata, the water table, or phreatic surface, forms the upper surface of the zone of saturation. This is defined as the surface of atmospheric pressure and appears as the level at which water stands in a well penetrating the aquifer. Actually, saturation extends slightly above the water table due to capillary attraction; however, water is held here at less than atmospheric pressure. Water occurring in the zone of saturation is commonly referred to simply as groundwater, but the term phreatic water is also employed.

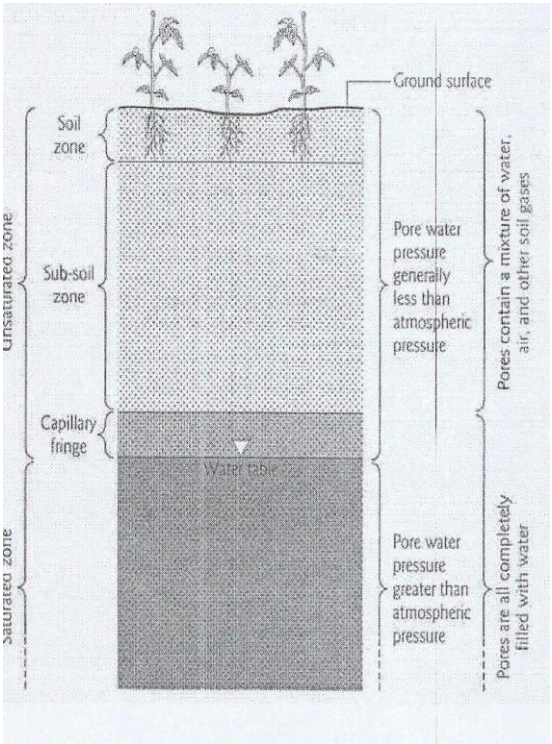


Figure 1.3: A schematic cross-section showing the typical distribution of subsurface waters in a simple "unconfined" aquifer setting, highlighting the three common subdivisions of the unsaturated zone and the saturated zone below the water table (Kevin, 2005).

1.1.4 Transmission of Groundwater

The dynamics of groundwater is mostly influenced by four hydrological processes. These are infiltration, recharge, leakage and withdrawal. These are processes through which groundwater is transmitted. Infiltration is the process of entry of surface water into the soil through ground surface. The rate of infiltration is defined as the volume of water entering into the ground surface through its unit cross-sectional area in unit time. The infiltration rate is known to vary with time which is initially decreases due to dispersion and swelling of soil particles after wetting (Alile and Amadasun, 2008). Then for a shorter period it increases due to the release of entrapped air from the pores. Thereafter, it decreases more or less in exponential form due to the clogging of the soil pores at the bottom of the surface reservoir. When the infiltration rate drops below a prescribed lower limit such that it is no more economical for aquifer recharging, then the infiltration operation is disconnected for some time. After drying, cleaning and if necessary scraping of the silty bottom of the recharge basin, infiltration is brought back to its almost initial value and the basin is put back to use for the next phase of the infiltration operation (Rear, 1979; Husiman and Olsthoorn, 1983; Dickenson and Bachman, 1995; Mousavi and Rezai, 1999).

1.1.5 Recharge

The process of entering of infiltrated water into the saturated zone. The rate of recharge is defined as the volume of water which enters into the saturated zone per unit cross sectional area and per unit time. This rate of recharge largely depends on the infiltration rate and follow pattern of variation more or less similar to that of infiltration rate with some time lag and less intensity. Just like infiltration rate is approximated the recharge rate can be approximated also by using linear element of different lengths and slopes depending on the nature of variation of recharge rates (Brown eta!., 1972).

1.1.6 Leakage

The leakage takes place between two adjacent aquifers through apportion of semi permeable boundary due to difference in hydraulic pressure. The leakage rate is defined as the volume of water leaving or entering the aquifers through a unit cross sectional area of semi permeable boundary in unit time (Bear, 2012). Leakage from an overlying or underlying aquifer with piezometric head, cD into aquifer with piezometric head C1 is given by:

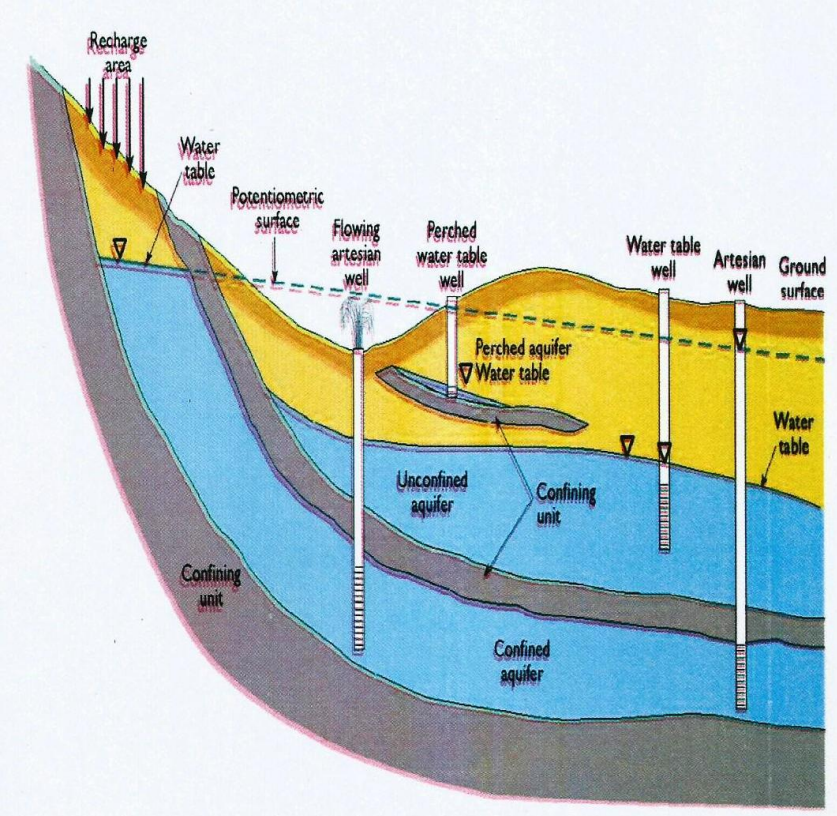
q ()(c_ c1) (Bear,2012) (1.1)

Where k and b are the hydraulic conductivity and thickness respectively of the semi permeable layer.

1.1.7 Aquifers

Aquifers are the geological formations which can store water as well as allow the flow of significant amount of water through their pores under ordinary field conditions. in these formations pores are interconnected to allow the flow of groundwater. Examples are sand, sandstone, weathered rocks, fractured rocks etc. If the aquifer is bounded by two impermeable formations from top and bottom is called a confined aquifer. Water level in a piezometer penetrating a confined aquifer is referred to s the piezometric surface. The pressure at the piezometric surface is equal to the atmospheric pressure. Water level in a well penetrating a confined aquifer represent piezometric surface. If the piezometric surface is above the ground surface, then a well located in this region will discharge groundwater on the ground surface without pumping. This segment of confined aquifer is known as artesian aquifer and the well is known as artesian well. If the upper boundary of the aquifer is the water table or phreatic surface is called an unconfined aquifer (Jochen and Mario, 2010). The pressure at the water table is equal to atmospheric pressure. The pressure above the water table is less than the atmospheric pressure whereas below the water table it is more than the atmospheric pressure. An unconfined aquifer or part of it that rest on a semi pervious layer is a leaky unconfined aquifer. Confined aquifer that has at least one semi pervious formation is called a leaky confined aquifer. Perched aquifers are special cases of unconfined aquifers in which a small impervious layer supports a groundwater body above the main water table. Different types of aquifers are shown in Figure 2.1. The same layer of an aquifer can represent different form of aquifers depending on the prevailing physical conditions. As shown in the Figure 2.4, the piezometric surface within the lower confined

aquifers segment falls below the top of the aquifer. In this segment, piezometric surface and water table coincides and the aquifers become unconfrned. Other than being the source of fresh water, aquifers are used for other purposes of groundwater resource management such as storage reservoir, as a filter for water of inferior quality injected into the aquifers etc. The geological formation that allows the flow of water at very low rate compare to the aquifer is called Aquitard. The formation that contains water but is incapable of transmitting significant quantities of groundwater under ordinary field conditions is referred to as Aquiclude. Clay is an example of aquiclude. The geological formation that neither store water nor allow the flow of water through them is called Aquifuge. Hard rock formations such as granites and basalts which are free from fractures, faults or weathering are example of Aquifuge.



igure 1.4: Hydrological cycle and aquifers type (Harlan *et al.*, 1989).

1.3 Statement of the Problem

The source of groundwater recharge from the U/rnai zanko well is not well understood. The focus of this research is to determine the source(s) of groundwater to the area surrounding the well. The focus of this research is to determine the source of groundwater and nature of extent of transmissivity to the area surrounding the well to know whether there is sufficient water for secondary use. Prior to exploring these water resources, the relationship between the local geology and hydrogeology must be understood in order to better characterize the aquifer system.

1.4 Aim and Objectives

The aim of this research work is to evaluate grand water potential of U/Mai Zanko. The objectives attainable in this study are to:

i) Characterise the subsurface based on its resistivity distribution

ii) Delineate thickness and depth to aquifer bearing rocks

iii) Delineate regions with high groundwater potential in the study area

1.5 Significance of the Study

Due to the pressing need for potable water for agricultural, domestic and industrial purposes

in the rural communities, any research aimed at the provision of this resource is worth undertaking. The uses of geophysical methods in the groundwater investigations will help reduce if not alleviate completely, the problem of borehole failures in the area. Hence boreholes drilled based on these geophysical investigations will yield utmost results for water yield thereby inhibiting the spread of water related diseases, promoting socio-economic activities thereby contributing to poverty alleviation and further increasing the life expectancy of the natives.

1.6 Scope of the Study

This project focuses on locating groundwater potential zones in Angwan Umai zanko. Groundwater exploration will be carried out in selected communities in the district. A total of thirteen communities will be considered in this study. Integrated geophysical tools, specifically the electrical resistivity methods will be used for the survey. The electromagnetic method will be

used as a reconnaissance survey tool. Profiling will be done with the Geonics EM 34-3 equipment. On the other hand, the resistivity method will be used to measure variations in the electrical resistivity of the ground with depth. Vertical electrical soundings (VES) based on the Schiumberger array system will be conducted at points indicated from the results of the electromagnetic profiling.

CHAPTER TWO

LITERATURE REVIEW

2.1 Previous Studies Carried Out

2D electrical resistivity method has developed greatly and has become an important instrument in hydrological studies, mineral prospecting and mining as well as in environmental and engineering applications (Griffiths et at., 1990; Griffiths and Baker, 1993; Dahlin and Loke, 1998; Olayinka, 1999; Olayinka Yararnanci, 1999; Amidu and Olayinka, 2006; Aizebeokhai et at., 2010). The underlying principle of measuring subsurface variation using electrical resistivity within the earth was developed by Schlumberger, who conducted the first experiment in 1912 in the field of Normandy and the same idea was also developed by Frank Wenner in the United State of America. (Kunetz, 1966). This electrical resistivity method has been found useful in locating groundwater in fissured rock, mapping of plumes, mapping of boundaries of saline groundwater and exploration of geothermal fluids (Kunetz, 1966).

Ayolabi et a!. (2009) used the electrical resistivity method for groundwater potential evaluation within the permanent site of the University of Agriculture, Abeokuta (UNAAB), Ogun State, Southwestern part of Nigeria. A total of 46 Schlumberger vertical electrical sounding (VES) stations were occupied using the ABEM Terrameter SAS 300B model with maximum inter-electrode spacing (AB) of 200 m.

Bale et al. (2010) investigated the geophysical and geotechnical assessment of the granite deposits at Idi-Osan Ofagada Village near Abeokuta, Southwestern Nigeria. Fourteen VES were carried out on the areas covered with overburden to determine their resistivity characteristics, overburden thickness and the reserve tonnage of the basement rock. The compressive strength and the specific gravity of the rock were also determined.

Badmus eta!. (2012) carried out lithological identification for groundwater prospects of three different locations in Abeokuta, Ogun State. The investigation involved the use of 3-Dimensional electrical resistivity model, with the help of the AREM SAS 30013 Terrameter. A manual 4-electrode system was used in the electrical resistivity tomography survey via the square array. The pole-pole array was used with the two remote electrodes placed at distances of

23 m, 40 m and 65 ni from the grids of I m, 3 m and 5 m unit electrode spacings respectively, to reduce their telluric effects on the measured apparent resistivity values.

Kowalska et at. (2012) detected groundwater pollution and identified the conditions of soil and groundwater near the coal waste disposal "Panewniki" Flalemba-Wirek Coal Mine using geoelectrical measurements. The first applied method was the VLF (Very Low Frequency) technique to delineate the preliminary contaminated zones, then followed by the electrical imaging method which was used to investigate the leachate plume.

Olurin et a!. (2012) analysed the physical parameters of Limestone Deposits in Ewekoro Formation, Southwestern Nigeria via direct laboratory method. The permeability, bulk density and resistivity values were obtained from the samples collected. The resistivity obtained was correlated with favorably with the results obtained from the electrical resistivity method of geophysical prospecting of the study area.

Adeoti et al. (2012) delineated and determined subsurface layers and groundwater potential respectively in Mowe, Ogun State, Nigeria using the Schlumberger Vertical Electrical Sounding. The study was carried out using the ABEM SAS 1000 terrameter which worked on 16 vertical electrical sounding (VES) points within the area. A maximum distance of 550m currcnt electrode spread was adopted for this survey revealing four geoelectric layers.

Ariyo et a?. (2013) investigated the effect of leachate contamination of groundwater using both Vertical Electrical Sounding (VES) and Constant Separation Traverse (CST) technique via Schiumberger and Wenner electrode configuration at Sotubo solid waste dumpsite along Sagamu-Ikorodu Road, Southwestern Nigeria.

Ogundana and Talabi (2014) used resistivity method to investigate the geoelectric characteristics of aquiferous units and its implication on groundwater potential of Northeastern part of Owo, Undo State. Thirty-two points were sounded adopting Schiumberger configuration along three different sections of the town; idasen, Okedogbon and Express. Six different subsurface lithologic units were established; lateritic topsoil, clay, sand, quartzite, weathered/fractured basement and, basement. The average resistivity and thickness values for the topsoil are 220 fm and 2.0 m respectively. Clay was encountered across Okedogbon and Express area of the town and the average resistivity and thickness values of 34 m and 6.0 m respectively. Sand was

encountered across the entire study area with average resistivity and thickness values of 115 m and 11.0 m respectively. Quartzite was encountered in all the locations with average resistivity and thickness values of 611 m and 11.0 m respectively. Weathered/fractured basement was encountered across the three sections with average resistivity and thickness values of 86 2m and 12.0 m respectively. Basement is relatively deep in the study area and the average resistivity and depth values to the top of basement are 878 m, and 24 m respectively. Overburden thickness was established across the area with an average value of 20 m. The overburden material with the fractured basement constitutes aquiferous units within the study area though the sand and weathered basement units are largely responsible for the groundwater potential. The groundwater potential of the area is moderate with express area having the highest potential.

Al-Hassan et al. (2015) used electrical resistivity method to survey groundwater at Eye Zheba village, off Bida- Minna road, Niger State, Nigeria. Schlumberger array method was employed, the area revealed three to five lithological formations which includes sandstone, clayey sandstone, sandy clay and ferruginised sandstone.

Adebayo et al. (2015) delineated contamination plumes at Olubonku Dumpsite at Ede Town, Osun State, Southwestern Nigeria with the view to assess the degree and extent of impact of the waste dumpsite on the quality of the groundwater in the study area. The investigation involved the electrical resistivity method via the Schiumberger Vertical electrical sounding, soil sampling analysis and hydrochemical analysis.

2.2 BASIC CONCEPTS OF ELECTRICAL RESISTIVITY METHOD

2.2.1 Vertical Electrical Sounding (VES)

In resistivity measurements using VES technique the measured parameters are: current injected into the ground and a voltage drop at a known electrode configuration. Often it is not easy to relate these measured quantities to resistivity stratification at the subsurface. To derive this relation many techniques have been employed, relying on several assumptions. It must be pointed out, however, that the determination of resistivity may solve an electric problem but not necessarily a geological one; the reason being that given geological formations are not associated with definite resistivities except in a broad and general manner (Parasnis, 1972).

The model which best describes many geological situations is that represented by an earth composed of a finite number of horizontal layers. Each layer is electrically homogeneous a swell as isotropic. The field is generated by a point current source at the surface, the current being direct current.

The basic equations for the derivation are:

$E = \beta J$ Ohm's Law (2.2)

$div\ J = 0$ Divergence condition (2.3)

where E=potential gradient; J = current density; ß =resistivity of the medium.

Combining the two equations,

$\nabla 2V = 0$ (2.4)

where V = potential .

Equation (2.4) can be solved by use of polar or cylindrical coordinates. Using the relationship

$$I = \int J.ds$$

it can be shown that for a single current source

$$v = \frac{ßI}{2\pi r} \quad (2.5)$$

For several sources of current the potential at any point on the surface is found by adding all the contributions of the current sources, since potential is a scalar. That is, potential at a point M is

$$V_m = \frac{ß}{2\pi}\frac{\Sigma I}{r} \quad (2.6)$$

and for potential at point N

$$V_n = \frac{ß}{2\pi}\frac{\Sigma I}{r} \quad (2.7)$$

21

where r is the distance between the current and potential electrode. However, in practice there are two current electrodes A and B (Figure 2.5). One being a source (positive) and the other *a* sink (negative) i.e.

$I_a = -I_b$

From the Schlumberger configuration, shown in Figure 2.5 it follows that

$$V_m = \frac{ßI}{2\pi}\left(\frac{1}{AM} - \frac{1}{BM}\right) \quad (2.8)$$

$$V_n = \frac{ßI}{2\pi}\left(\frac{1}{AN} - \frac{1}{BN}\right) \quad (2.9)$$

The potential difference divV across MN is then

$$V_m - V_n = \frac{ßI}{2\pi}\left(\frac{1}{AM} - \frac{1}{BM} - \frac{1}{AN} + \frac{1}{BN}\right) \quad (2.10)$$

Simplifying,

$$: divV = \beta IK \quad (2.11)$$

where K is known as the geometric factor depending on the electrode configuration. In the Schlumberger array AM=NB and, designating

AB/2 = s

MN/2 = p

it can be shown that

$$ß = \frac{divV}{I}\frac{\pi}{2}\frac{(s^2 - p^2)}{p} \quad (2.12)$$

or

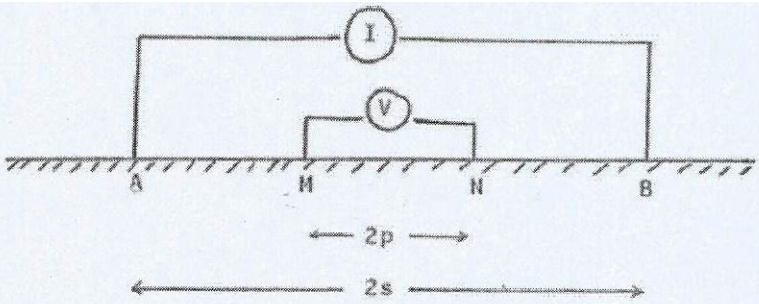


Figure 2.1: The Schlumberger array configuration (Telford *et al.*, 1990)

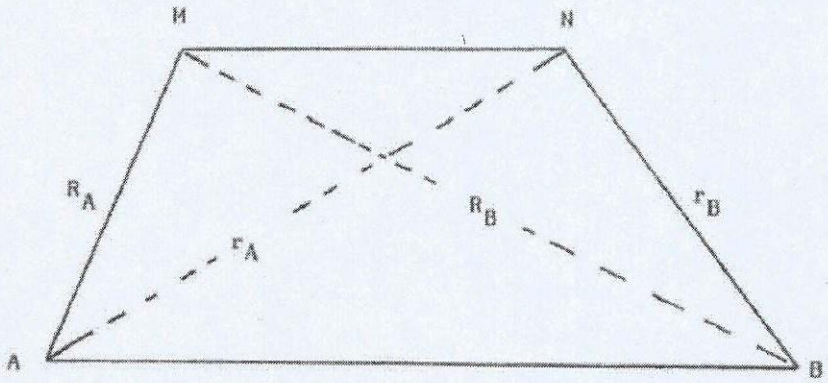


Figure 2.2: General four electrode array (Telford *et al.*, 1990).

$$ß = \frac{divV}{I} K_s$$

K_s being the geometric factor for the Schlumberger array. Since the earth is not homogeneous ß is not the true resistivity but the apparent resistivity, $ß_a$ which may be larger or smaller than, or in rare cases identical with, one of the resistivity values in the heterogeneous earth. Therefore,

$$ß_a = \frac{divV}{I} K_s \qquad (2.13)$$

In the field, parameters are divV and I. However, divV, the potential gradient, cannot be determined exactly, since it is defined as the limit of the ratio of the voltage to spacing as the two potential electrodes, MN, move closer together. The error introduced into the resistivity

by having a measurable MN can be evaluated. Keller et al. (1970) have shown that in order to keep the apparent resistivity within a given error limit, say e, the following relation must be satisfied.

$$p^2 = \frac{4e}{1+e} s^2 \qquad (2.14)$$

For Schlumberger Sounding it is desirable to use e=5 percent, which means that,

$$p \leq 0.435s \qquad (2.15)$$

2.2.2 2D Electrical Resistivity Theory

All resistivity methods employ an artificial source of current which is introduced into the ground through point electrodes or long line contacts. The procedure is to measure potentials at other electrodes in the neighborhood of the current flow. Electrical methods of geophysical investigations are based on the resistivity or its inverse (i.e.) conductivity of materials. The electrical resistance, R of a material is related to its physical dimension, cross sectional area, A, length, L, through the resistivity ρ or its inverse, conductivity, σ is given by

$$\rho = \frac{1}{\sigma} = \frac{RA}{L} \qquad (2.16)$$

Low frequency alternating current is employed as source signals in the DC resistivity surveys in determining subsurface resistivity distribution. Usually a complete homogeneous and isotropic is considered. For homogeneous medium, the current density J and electric field E are related through Ohm's law.

$$J = \sigma E \tag{2.17}$$

Where E is in volts per meter and σ is the conductivity of the medium in Siemens per meter (m).

The electric field E can be represented as gradient of a scalar potential

$$E = \nabla V \tag{2.18}$$

$$J = \sigma \nabla V \tag{2.19}$$

But $\nabla . J = 0$, $\nabla . (\sigma \nabla V) = 0$

By combining equations 2.16 and 2.17, we obtained fundamental Laplace's equation for electrostatic fields which is given by

$$\nabla^{P2} V = 0 \tag{2.20}$$

2.2.2.1 Single Current Electrode at Depth

There are several field configurations used in resistivity. The first of these is the electrode of small dimensions buried in a homogeneous isotropic medium. This is where the single electrode is down a drill hole or otherwise under the ground. The current circuit is completed through another electrode usually at surface, but in any case, far enough away that its influence is negligible.

From the symmetry of the system the potential will be a function of r only, where r is the distance from the first electrode. Under these conditions Laplace's in spheric coordinate is given by:

$$\nabla^2 V = \frac{\partial^2 v}{\partial r^2} + \left(\frac{2}{r}\right)\frac{\partial v}{\partial r} = 0 \qquad (2.21)$$

Multiplying equations 2.20 by r^2 yield,

$$\frac{\partial v}{\partial r} = \frac{A}{r^2} \qquad (2.22)$$

On integrating, equation 2.22 yields,

$$V = -\frac{A}{r} + B \qquad (2.23)$$

Where A and B are constant.

When the current flows radially outward in all direction from the point electrode, the total current crossing a spherical surface is given by

$$I = 4\pi r^2 J = -4\pi r^2 \sigma \frac{\partial v}{\partial r} = -4\pi\sigma A \qquad (2.24)$$

Combining (2.20) and (2.17), yields

$$A = \frac{I\rho}{4\pi}$$

Hence,

$$V = \frac{\rho I}{4\pi r} \; or \; \rho = \frac{4\pi V r}{I} \qquad (2.25).$$

2.2.2.2 Single Current Electrode at the Surface

If the point electrode delivering current is located at the surface of the homogeneous isotropic medium, the single probe or three points system is used in surface resistivity layout and the return current electrode is at a great distance.

By applying Laplace's equation, the solution will be

$$V = -\frac{A}{r} + B \text{ With } \quad B = 0 \tag{2.26}$$

The current flows through a hemispherical surface in the lower medium is given by

$$V = \frac{\rho I}{2\pi r} \; or \; \rho = \frac{2\pi V r}{I} \tag{2.27}$$

2.2.2.3 Two Current Electrodes at the Surface

When the distance between the two current electrodes is finite, the potential

$$V_1 = -\frac{A_1}{r_1} \qquad \text{Where,} \qquad A_1 = -\frac{I\rho}{2\pi}$$

The potential due to C_2 at P_2 is

$$V_2 = -\frac{A_2}{r_2} \text{Where} A_2 = -\frac{I\rho}{2\pi} = A_1$$

Thus,

$$V_1 + V_2 = \frac{I\rho}{2\pi}\left(\frac{1}{r_1} - \frac{1}{r_2}\right) \tag{2.28}$$

Introducing a second potential electrode at P2, the difference in potential between P1 and P2 can be measured which is given by

$$\Delta V = \frac{I\rho}{2\pi}\left(\frac{1}{r_1} - \frac{1}{r_2}\right) - \left(\frac{1}{r_3} - \frac{1}{r_4}\right) \quad (2.29)$$

2.2.3 Apparent Resistivity and Electrode Configuration

The purpose of electrical survey is to determine the subsurface resistivity distribution by making measurements on the ground surface. From these measurements, the true resistivity of the subsurface can be estimated. The ground resistivity is related to various geological parameters such as the mineral and fluid content, porosity and degree of water saturation in the rock. Electrical resistivity surveys have been used for many decades in hydrogeological, mining and geotechnical investigations. More recently, it has been used for environmental surveys.

The resistivity measurements are normally made by injecting current into the ground through two electrodes (C1 and C2) in Fig (2.7), and measuring the resulting voltage difference at two potential electrodes (P1 and P2).

From the current (I) and Voltage (V) values, an apparent resistivity (ρa) value is calculated.

$$\rho a = K\frac{V}{I} \quad (2.30)$$

Where k is the geometric factor which depends on the arrangement of the four electrodes. The Figure (2.8) shows the common arrays used in resistivity surveys together with their geometric factors. Resistivity meters normally give a resistance value, $R = \frac{V}{I}$, so in practice the apparent resistivity value is calculated by

$$\rho_a = KR \quad (2.31)$$

The calculated resistivity value is not the true resistivity of the subsurface, but an "apparent" value which is the resistivity of a homogeneous ground which will give the same resistance value for the same electrode arrangement. The relationship between the "apparent" resistivity and the "true'' resistivity is a complex relationship. To determine the true subsurface resistivity, an inversion of the measured apparent resistivity values using a computer program software package has to be carried out (Loke, 1997).

2.2.4 Resistivity Surveys

The resistivity method has its origin in the 1920's due to the work of the Schlumberger brothers. For approximately the next 60 years, for quantitative interpretation, conventional sounding surveys (Koefoed, 1979) were normally used. In this method, the center point of the electrode array remains fixed, but the spacing between the electrodes is increased to obtain more information about the deeper sections of the subsurface.

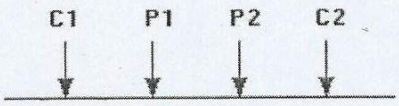


Figure 2.3: A conventional four electrode array to measure the subsurface resistivity.

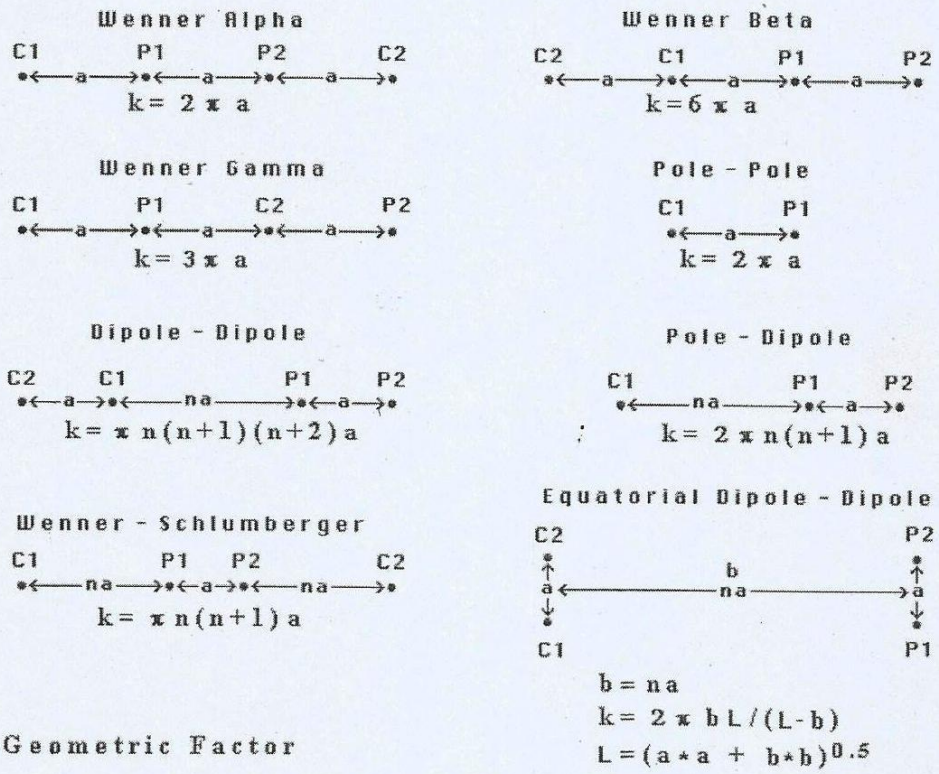


Figure 2.4: Common arrays used in resistivity surveys and their geometric factors (Loke, 1997, 1999).

2.2.4.1 Dipole-Dipole Array Configuration

In the acquisition of data, the dipole-dipole electrode array consists of two sets of electrodes, the current (source) and potential (receiver) electrodes. A dipole is a paired electrode set with the electrodes located relatively close to one another; if the electrode pair is widely spaced it is referred to as a dipole. The convention for the dipole-dipole electrode array (Figure 2.9) is to maintain an equal distance for both the current and the potential electrodes (spacing = a), with the distance between the current and potential electrodes as an integer multiple of a. The electrodes do not need to be located along a common survey line.

A primary advantage of the dipole-dipole electrode array is the ease of deployment in the field due to shorter wire lengths. However, a large generator may be needed to transmit a greater current magnitude for the measurement, especially for deep soundings

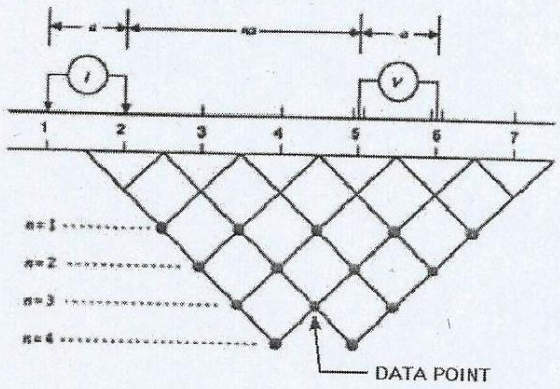
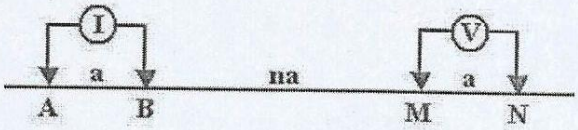


Figure 2.5: Dipole -Dipole Array Configuration (Loke, 1999).



$$\rho_A = \frac{V}{I}\pi a\, n(n+1)(n+2).$$

Figure 2.6: Dipole-Dipole Array Configuration (Milsom, 1996).

2.2.4.2 Pole-Dipole Array Configuration

The pole-dipole array contains four collinear electrodes. One of the current (source) electrodes is installed at an "effective infinity" distance, which is approximately five to ten times the survey depth. The other current electrode is placed in the vicinity of the two potential (receiver) electrodes. This geometry is utilized because it reduces the distortion of equipotential surfaces (Smith, 1986).

electrodes makes this array an attractive alternative. The signal strength for the pole-dipole array decreases with the *square* of the "**n**" factor. While this effect is not as severe as the dipole-dipole array, it is usually not advisable to use "**n**" values of greater than 8 to 10. Beyond this, the "**a**" spacing between the P1-P2 dipole pair should be increased to obtain a stronger signal strength (Loke, 1997).

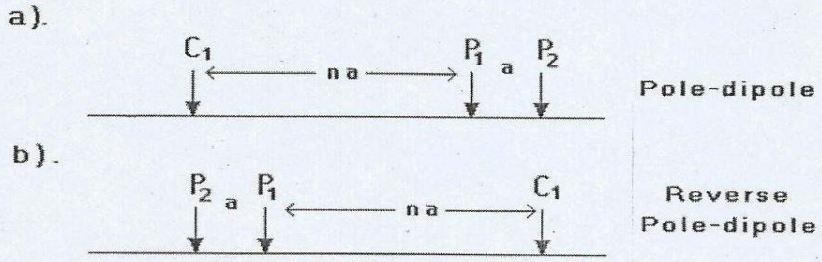


Figure 2.7: The forward and reverse pole-dipole arrays.

The resistivity is thus stated in equation (2.31):

$$\rho_a = 2\pi n\,(n+1)\,a\,\frac{v}{I} \qquad (2.32)$$

The pole-dipole array also has relatively good horizontal coverage, but it has a significantly higher signal strength compared with the dipole-dipole array and it is not as sensitive to telluric noise as the pole-pole array. Unlike the other common arrays, the pole-dipole array is an asymmetrical array (Figure 2.7a) and over symmetrical structures the apparent resistivity anomalies in the pseudo-section are asymmetrical. In some situations, the asymmetry in the measured apparent resistivity values could influence the model obtained after inversion. One method to eliminate the effect of this asymmetry is to repeat the measurements with the electrodes arranged in the reverse manner (Figure 2.7b). By combining the measurements with the "forward" and "reverse" pole-dipole arrays, any bias in the model due to the asymmetrical nature of this array woul4 be removed.

The pole-dipole array also requires a remote electrode, the C2 electrode, which must be placed sufficiently far from the survey line. For the pole-dipole array, the effect of the C2 electrode is approximately proportional to the square of ratio of the CI-Pi distance to the C2-Pl distance. Thus the pole-dipole array is less affected by the C2 remote electrode compared with the pole-pole array. If the distance of the C2 electrode is more than 5 times the largest Ci-PI distance used, the error caused by neglecting the effect of the C2 electrode is less than 5% (the exact error also depends on the location of the P2 electrode for the particular measurement and the subsurface resistivity distribution).

Due to its good horizontal coverage, this is an attractive array for multi-electrode resistivity meter systems with a relatively small number of nodes. The signal strength is lower compared with the Wenner and Wenner-Schlumberger arrays but higher than the dipoledipole array. For IP surveys, the higher signal strength (compared with the dipole-dipole array) combined with the lower EM coupling (compared with the Wenner and WennerSchlumberger arrays) due to the separation of the circuitry of the current and potential

CHAPTER THREE

MATERIALS AND METHODS

3.1 Data Acquisition

In carrying out electrical resistivity survey, Plate 1 shows PASI Terrameter, alongside with an external battery (12 V. 60 Ah Battery), one Global Positioning System (GPS), four metal electrodes, four pieces of hammer, four reel of cables, measuring tape were used for the resistivity measurements. The four electrodes were pegged along the profile of six (6) traverses by using a measuring tape to measure the electrode spacing of 5 m and also made sure it was in a straight line. The electrodes were driven into the soil with the aid of hammer and the electrode-cables were clipped to the electrode using crocodile clips and the cables were connected to the terrameter powered by a battery, placed at the mid-point and shielded with an umbrella to prevent sun rays from getting to the terrameter and external battery. Then readings were taken with each electrode spacing while the terrameter system checked if the electrodes were well connected before readings commenced. The coordinates of each of the traverse line and specific points for the VES were taken with a GPS.

3.2 Schlumberger Array

Thirty Vertical Electrical Sounding stations were acquired at major points, as shown in Figure 2.5. The geodetic system of coordinates was obtained using Garmin 12 Global Positioning System. The Schlumberger current electrode separation (AB) was varied from a minimum of 2 to 400 m. Five VES points were established o each profile.

3.2.1 Two dimensional (2D) resistivity imaging

The Wenner array electrode was used for the 2D resistivity imaging data acquisition. This electrode configuration is well suited for constant separation data acquisition systems, so that many data-points cati be recorded simultaneously for each current injection. A 2D resistivity

survey was carried out using the PASI Terrameter. Measurements were made at sequences of electrodes at 5 m, 10 m, 15, 20 m, 25 m and 30 m interval using four (4) electrodes for all the six traverses covering a distance between 180 m and 200 m each.

3.3 Data Processing/Interpretation

3.3.1 Vertical Electrical Sounding

3.3.1.1 Qualitative And Qualitative Analysis

The qualitative interpretation of the depth sounding curves was carried out based on individual eo-electric characteristics on the number of layers represented by the four type of the auxiliary curves (A, H, K, and Q) and also from the profiles and maps involves inspection for patterns/anomaly signatures that are diagnostic of the target.

The quantitative interpretation of the depth sounding curves was cried out by adopting the partial curve matching technique (Rhattachary & Patra, 1968). In order to this, the VES data were plotted on a transparent overlay. The partial curve matching technique involved the use of a standred two (2) layer master curve and four (4) auxiliary types curves (H, K, A, & Q). This procedure required segment-by-segment curve matching starting from the position with shorter electrode spacing and moving towards those with longer spacing.

The result of the VES curves obtained from the partial curve matching were than used to constrain the interpretation by the computer using iteration software known as WinResist Software. This invariably reduces overestimation of depths. The result of the computer iteration sbows the quantitative analysis to know the resistivity, thickness and depth.

The difference between measured and observed gives the inversion model which represents the geology of the study area.



Plate 1: PASI 16GL (Resistivity Meter) and its Accessories

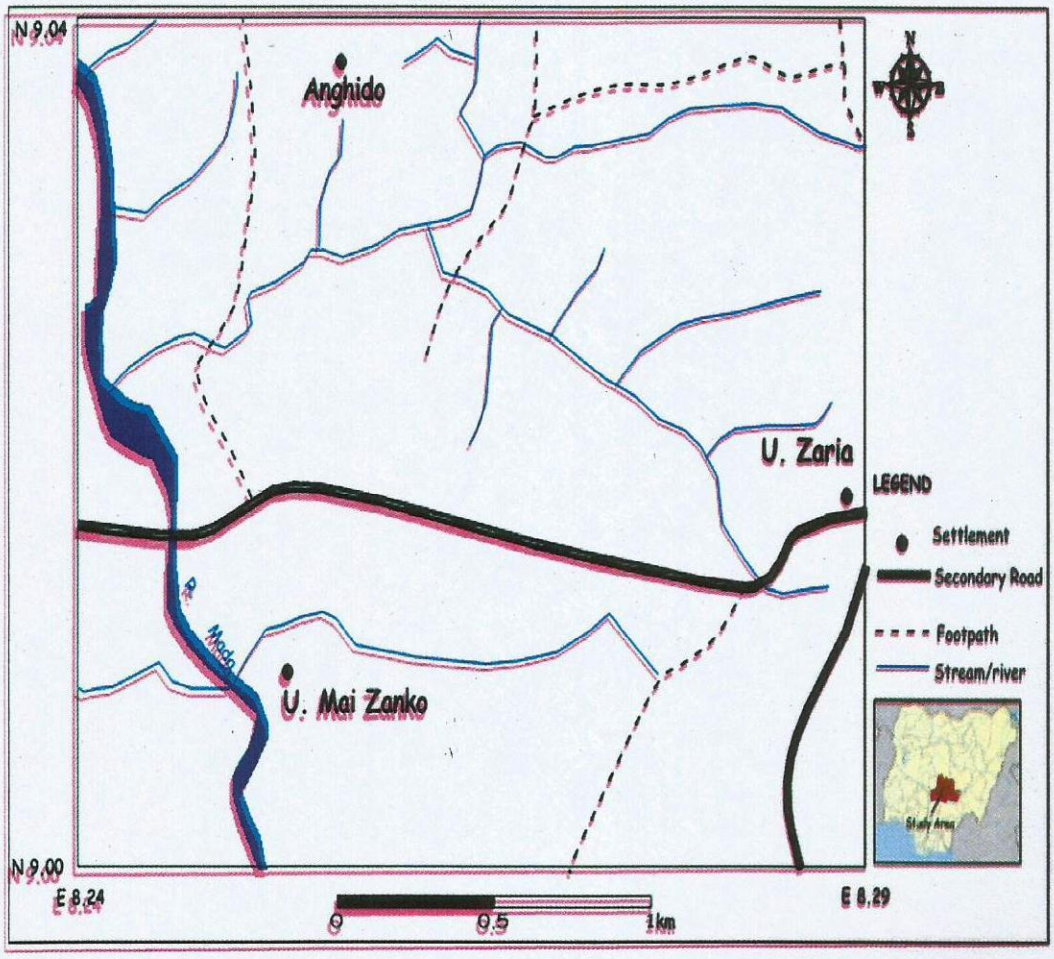


Figure 3.1: Location Map of the Area

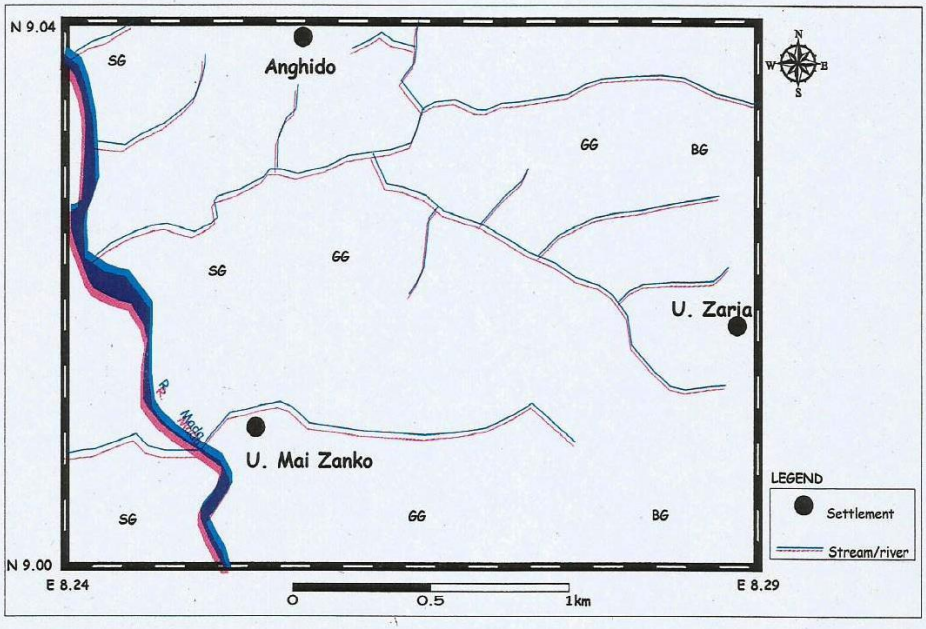


Figure 3.2: Drainage Map of the Area

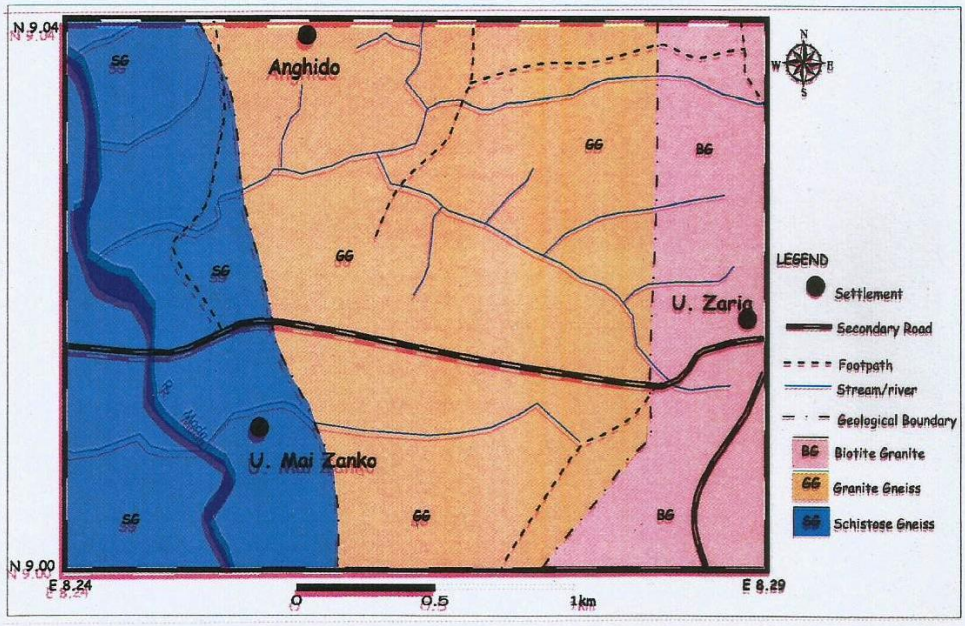


Figure3.3: Geological Map of the Area

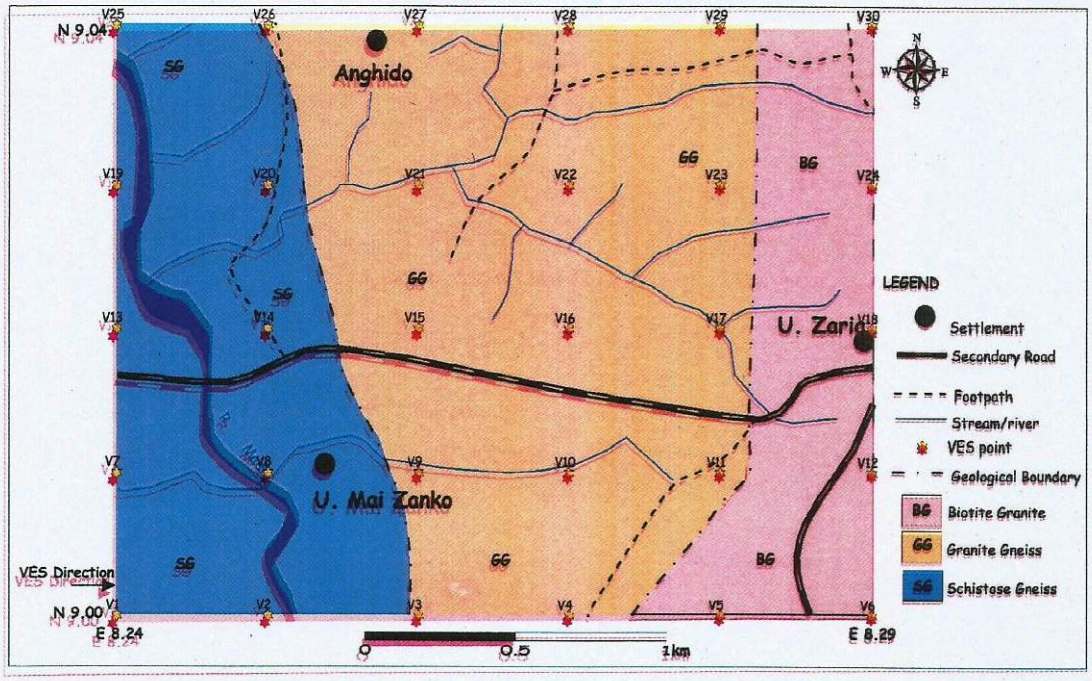


Figure3.4: Geological Map with VES Points

CHAPTER FOUR

RESULTS AND DISCUSSION

The results of vertical electrical sounding (VES) are often interpreted quantitatively as a series of curves using computer assisted iterative software packages, also as a series of contour map when using gridded data. The lPl2win software package (Aleixei, 2002) was used to produce the curves from the field data while the contouring package surfer 12 was used to produce the maps from the values obtained from the curves.

4.1 Fjeld curves

The result of the thirty (30) VES carried out in the study area showed that the subsurface is made up of a maximum of five (5) layers and a minimum of three (3) layers. The four layer case dominate with twenty-three (23) VES stations exhibiting four layer case scenarios, followed by the five layer case with four (4) and the three layer case with three (3). The layers have been interpreted to consist of the top layer, lateritic layer, weathered layer and the fresh basement. The four layer case is characterised by the absence of the lateritic layer, while the three layer case consist only of the top layer, weathered layer and the fresh basement. The result of the VES across the area is summarised in table 4.1.

Also, six (6) different curve types have been identified in the area based on the number of layers. These include the H, HA, Qil, KH, QHA and KQH curve types. The QH curve type dominate with thirteen (13), representing 43.33% of the curve types, followed by the KH with nine (9), representing 30%, the H and the KQH have three (3) each representing 10% each rind the HA and QHA have one (1) each representing 3.3 3% each of the total curve types. The characteristic curve type in each VES station are summarised in table 4.2. The representative curve types in the area are shown in figures 4.1 to 4.6.

Table 4.1 Summary of VES result across the study area

VES No.	ρ1	ρ2	ρ3	ρ4	ρ5	T1	T2	T3	T4	d1	d2	d3	d4	Curv Type
1	2063	1707	255	129078	-	0.90	7.88	9.96	-	0.90	8.78	18.7	-	QH
2	2640	2090	311.1	204976	-	0.81	8.30	10.2	-	0.81	9.10	19.3	-	QH
3	6347	1568	464.3	19554	-	2.09	6.37	11.1	-	2.09	8.47	19.5	-	QH
4	5883	657.8	3096	61496	-	2.77	7.83	31.8	-	2.77	10.6	42.5	-	HA
5	8705	3309	729.3	5152	-	0.74	1.32	9.19	-	0.74	2.05	11.2	-	QH
6	10657	1726	366.7	2149	21842	0.63	2.92	4.04	17.6	0.63	3.55	7.59	25.2	QHA
7	1400	3175	561.3	294206	-	2.04	5.27	8.96	-	2.04	7.32	16.1	-	KH
8	2334	9791	328.3	803253	-	1.80	2.11	4.58	-	1.80	3.91	8.49	-	KH
9	541.6	2184	407.8	319.8	32275	0.71	0.98	10.7	27.3	0.71	1.70	12.4	39.7	KQH
10	1020	3616	122.2	57110	-	2.49	2.04	15.1	-	2.49	4.53	19.6	-	KH
11	1786	6732	1160	371.6	26093	0.90	1.02	6.85	31.3	0.90	1.92	8.77	40.0	KQH
12	593.9	1846	114.6	32372	-	2.16	2.21	13.8	-	2.16	4.37	18.2	-	KH
13	1654	4377	1011	480906	-	2.43	2.86	12.4	-	2.43	5.29	17.7	-	KH
14	540.8	922.6	140.6	34343	-	0.48	3.20	15.4	-	0.48	3.68	19.1	-	KH
15	1680	8163	1715	247.3	121978	0.71	0.83	8.95	17.3	0.71	1.54	10.5	27.8	KQH
16	146.3	552.4	124.4	1896	-	1.10	4.22	14.1	-	1.10	5.32	19.4	-	KH
17	149.4	1529	110.3	36643	-	1.66	2.06	14.1	-	1.66	3.72	17.8	-	KH
18	110.7	1162	51.18	41876	-	0.78	3.39	4.69	-	0.78	4.17	8.86	-	KH
19	2182	386.1	48.72	1185	-	1.57	7.87	9.71	-	1.57	9.44	19.2	-	QH
20	6523	956.6	80.47	685.5	-	0.55	2.27	6.01	-	0.55	2.82	8.82	-	QH
21	2303	1087	582.3	2335	-	1.92	6.85	31.4	-	1.92	8.77	40.2	-	QH
22	1082	244	2765	-	-	1.94	21.5	-	-	1.94	23.5	-	-	H
23	1667	504.9	98.01	12123	-	0.72	1.49	2.24	-	0.72	2.21	4.45	-	QH
24	1913	559.2	140.3	150924	-	0.65	3.64	4.55	-	0.65	4.28	8.83	-	QH
25	5676	810.5	116.5	9960	-	0.63	2.07	17.6	-	0.63	2.71	20.3	-	QH
26	3062	1575	92.41	1049	-	0.81	1.10	9.37	-	0.81	1.91	11.3	-	QH
27	2168	537.3	16119	-	-	2.70	10.0	-	-	2.70	12.7	-	-	H
28	2195	827.7	222.1	952.4	-	1.39	3.77	17.2	-	1.39	1.765	22.4	-	QH
29	3340	1396	538.4	4006	-	0.54	1.22	14.3	-	0.54	1.76	16.0	-	QH
30	3256	115	40088	-	-	1.98	11.6	-	-	1.98	13.6	-	-	H

ρ1 - ρ5 are the resistivity of the 1st – 5th layer respectively, T1 – T4 are the thicknesses of the 1st – 4th layer respectively and d1 – d4 are the depth of the 1st – 4th layer respectively

Table 4.2 Characteristic curve types in the area with their frequency and percentage

S/No	Curve Types	Curve Characteristics	Curve Frequency	% Curve Type
1	H	ρ1> ρ2< ρ3	3	10
2	HA	ρ1> ρ2< ρ3< ρ4	1	3.33
3	QH	ρ1> ρ2> ρ3< ρ4	13	43.33
4	KH	ρ1< ρ2> ρ3< ρ4	9	30
5	QHA	ρ1> ρ2> ρ3< ρ4< ρ5	1	3.33
6	KQH	ρ1< ρ2> ρ3> ρ4< ρ5	3	10

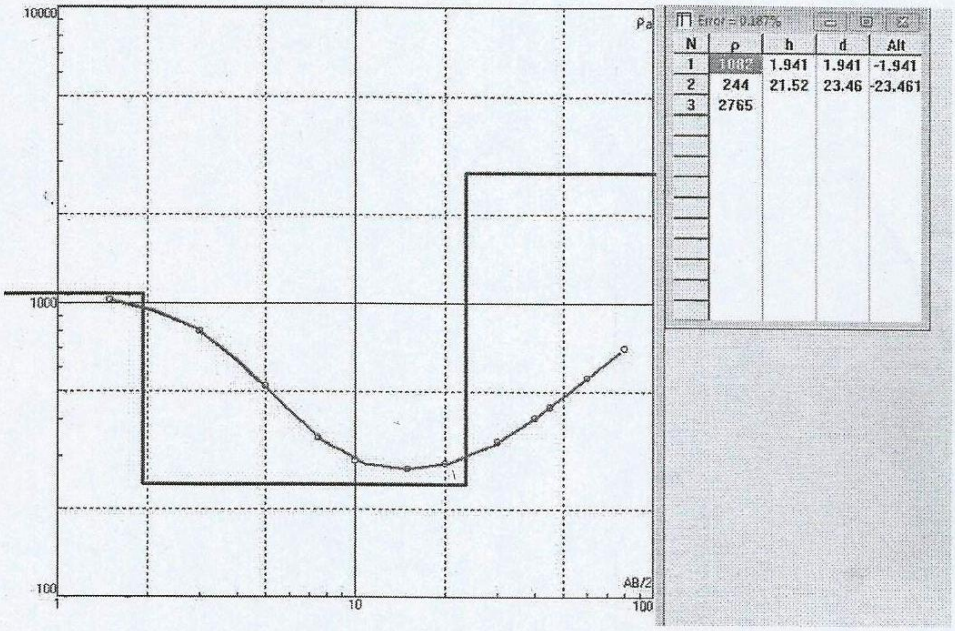


Figure 4.1 Typical H-type curve in the study area

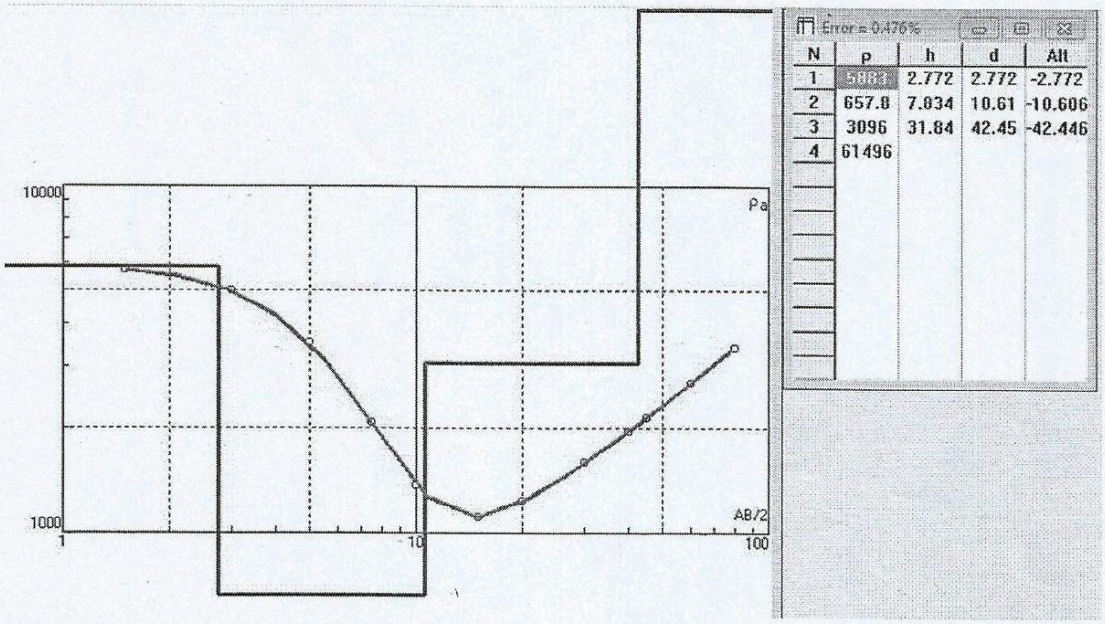


Figure 4.2 Typical HA-type curve in the study area

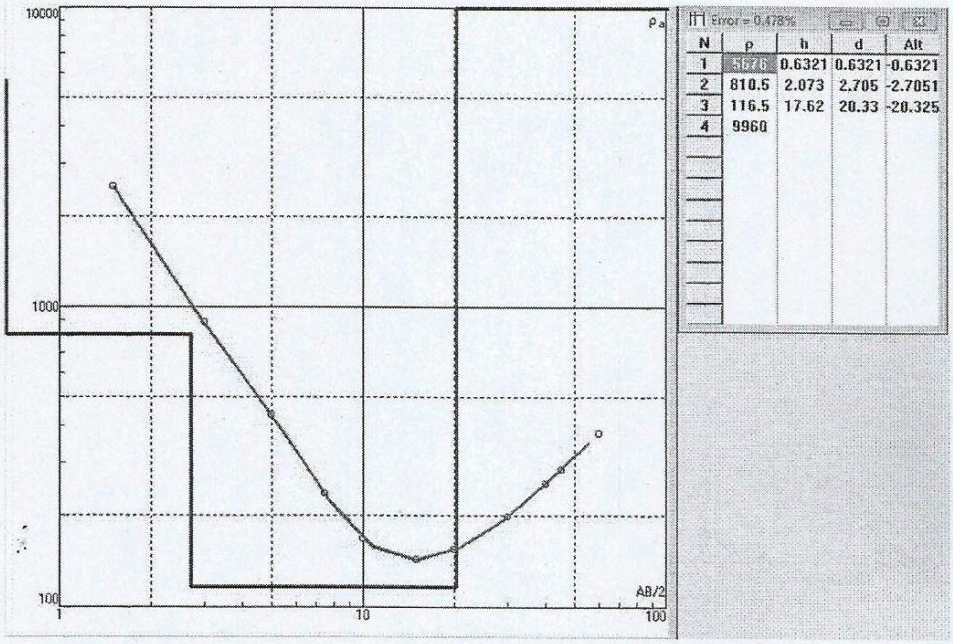


Figure 4.3 Typical QH-type curve in the study area

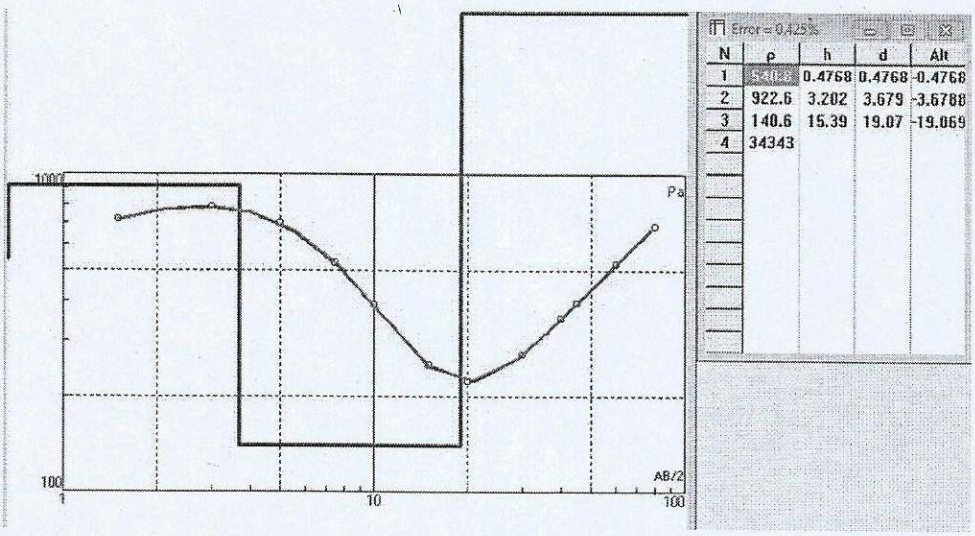


Figure 4.4 Typical KH-type curve in the study area

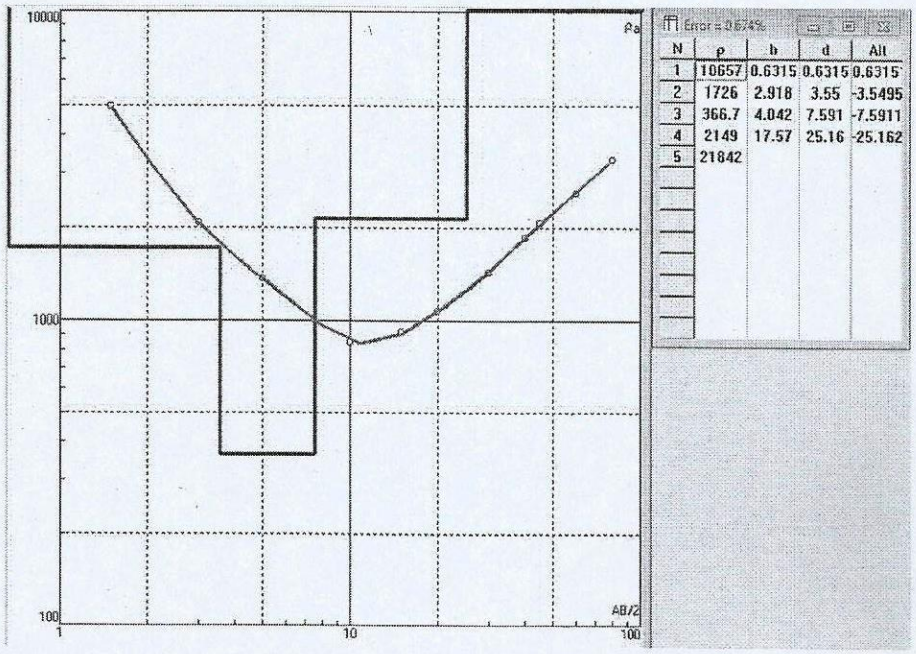


Figure 4.5 Typical QHA-type curve in the study area

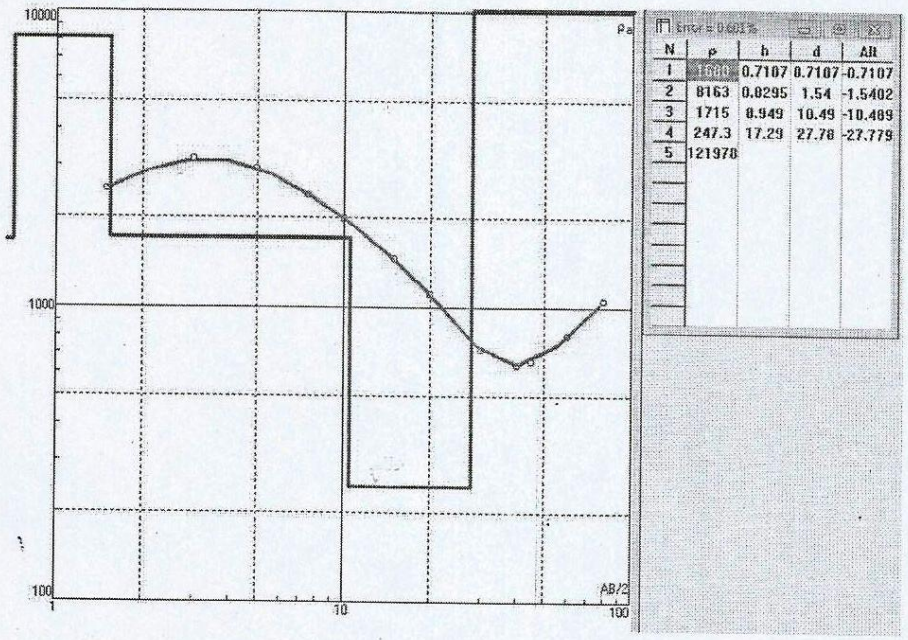


Figure 4.6 Typical KQH-type curve in the study area

4.2 Top layer resistivity

The top layer resistivity values across the VES stations vary between 110.7 m and 10657)m, with an average of 2733.6 2m. The values of the top layer resistivity were obtained by taking the resistivity of the first layer in each VES station. Higher resistivity values may indicate area with surface or near surface basement exposures, while lower resistivity values may indicate areas with considerable soil or sediment thickness probably aided by higher degree of weathering. Low top layer resistivity may also be indicative of water logged or swampy area. The 2D top layer resistivity contour map (figure 4.7) shows that the north-western and the southern to south-eastern portions of the map typified by brownish-yellow colouration have higher top layer resistivity while the bluish area around the central portion of the map have lower top layer resistivity.

4.3 Overburden thickness (depth to basement)

The overburden thickness map, also known as the isopach map is the depth to fresh basement in the area. It is made up of all the layers from the top layer to the fractured layer. This was obtained by compiling the values of the depth to basement in all the VES stations. Higher overburden thickness indicates higher groundwater potential as aided by higher degree of weathering in the area and vice versa for area with lower overburden thicknesses. The depth to basement in the study area ranges from 4.45 m to 40.2 m with an average of 18.76 m. This quite agrees with the work of Jatau et al., (2013) who predict depth of between 15 m —49 m in the North-Central Nigerian Basement Complex. The 2D overburden thickness map (figure 4.8) shows that the central to south-eastern portion of the area has higher overburden thicknesses typified by brownish colouration as against the western and the north-eastern portions of the study area with bluish colourations.

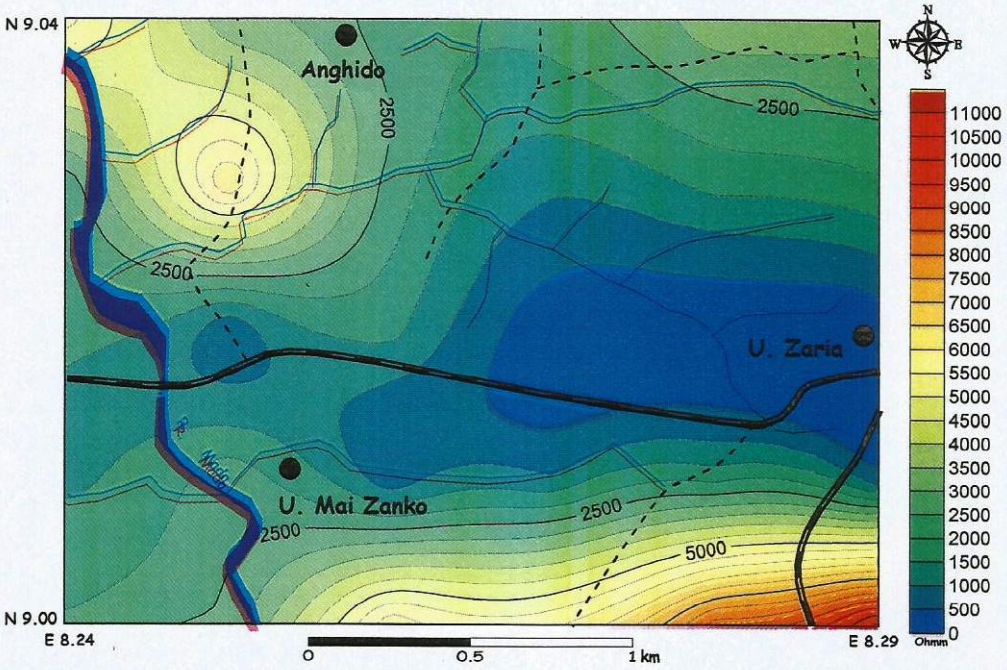


Figure 4.7 Top layer resistivity map

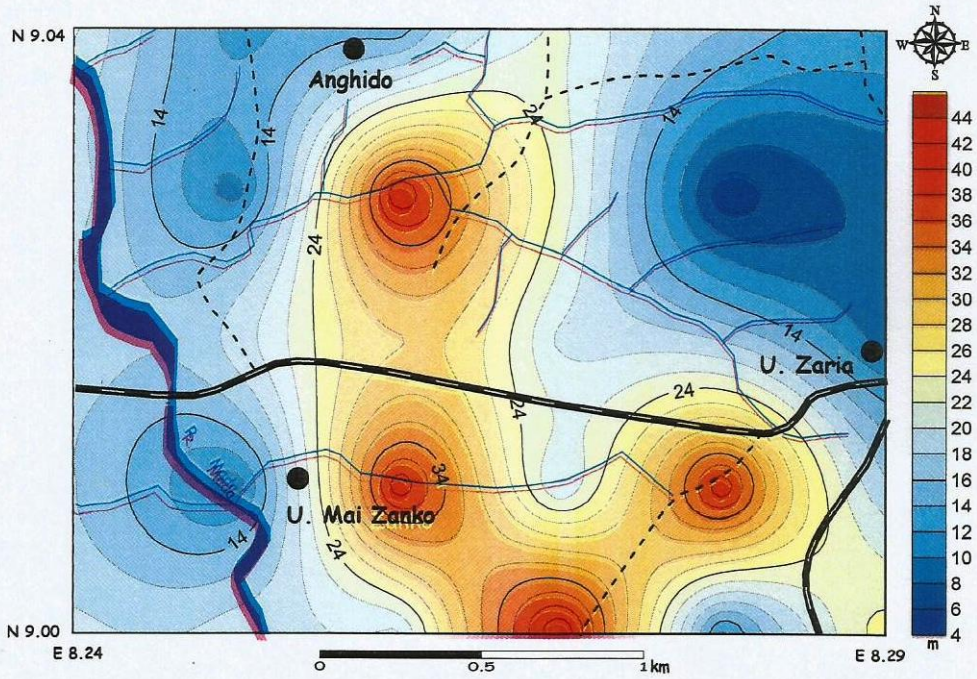


Figure 4.8 Overburden thickness map

4.4 True aquifer resistivity

The true aquifer was determined, taking into cognisance the resistivity of the layer interpreted as the potential aquifer, the thickness and depth of occurrence of the layer. Lower resistivity with good thickness and depth represent a good groundwater potential layer. The resistivity values for each of the layer considered to be the potential aquifer were used to plot the true aquifer resistivity contour map (figure 4.9). The true aquifer resistivity varies between 48.7 m and 729.3 fIm with an average of 310.6 c2m across the area. The goldingbrown colourations on the true aquifer resistivity contour map show areas of low resistivity, around the eastern and north-western portion.

4.5 True aquifer thickness A This was obtained by taking the thickness values of the layers considered to be the potential

aquifers. This was contoured to produce the true aquifer thickness map (figure 4.10). The true aquifer thickness ranges from 2.2 m to 31.4 m with a average of 12.06 m across the study area. The higher the thickness of the aquifer, the better the groundwater potential of the aquifer.

4.6 Groundwater potential zone

The groundwater potential of the study area (figure 4.11) has been categorised into three zones — Good, Moderate and poor. The groundwater potential zones were categorised based on the resistivity and thickness of the weathered layer (true aquifer) and the overburden thickness. A good groundwater potential zone should have low resistivity with considerable thickness and laying in a thick overburden zone. The zone with low true aquifer resistivity (100 flm-300 m), with true aquifer thickness of about 10 m and above and overburden thickness of about 15 m and above was considered to be a good groundwater potential zone.

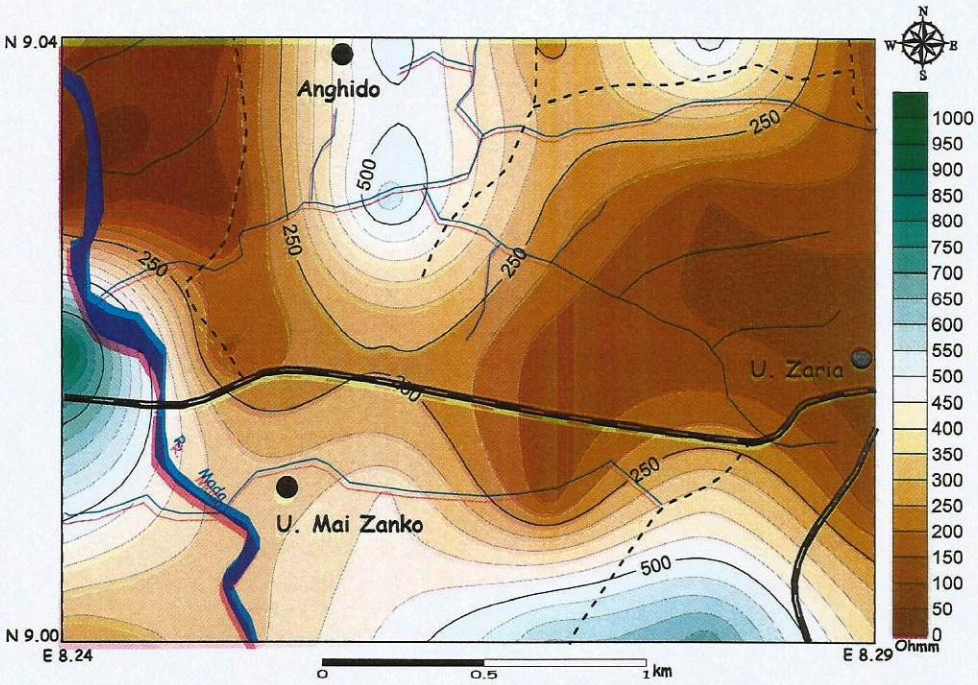


Figure 4.9 True aquifer resistivity map

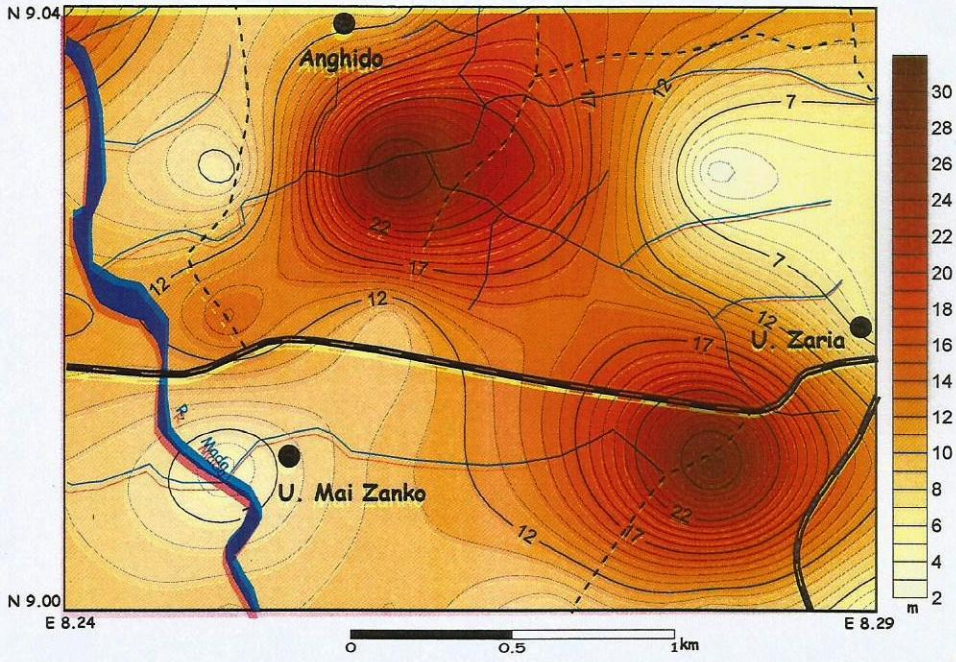


Figure 4.10 True aquifer thickness map

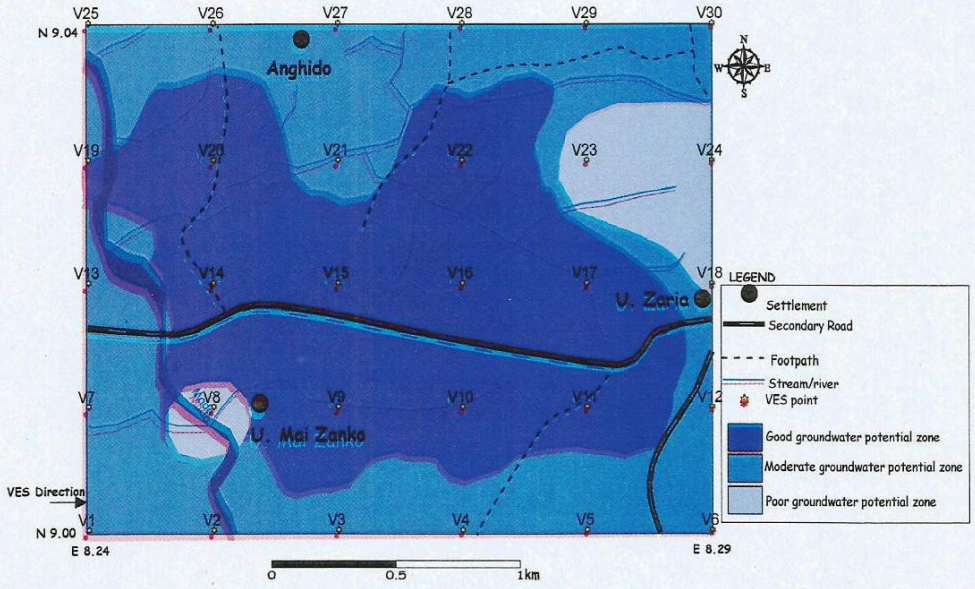


Figure 4.11 Map of groundwater potential zones

The resistivity of the moderate groundwater potential zone on the other hand is put at between >300 m - 1000 m, with thickness range of between <10 m to 7 m. The poor groundwater potential zone was isolated by virtue of its low thickness (<7 m). Ameloko & Rotimi (2010) and Lenkey *et al.,* (2005), stated that the large thickness of weathered material over-laying the basement rocks constitute a good aquifer in the Basement Complex terrain.

CHAPTER FIVE

SUMMARY, CONCLUSION AND RECOMMENDATION

5.1 Summary

Geophysical survey to evaluate the groundwater potential of Ungwan Mai Zanko and environs bounded by latitudes N 9.00-N 9.04 and longitudes E 8.24-E8.29 in Akwanga Local Government Area of Nasarawa State, located within the Basement Complex of Central Nigeria was carried out.

Thirty (30) VES were conducted on gridded profiles, employing the schlumberger array configuration, using omega resistivity metre and its accessories with a maximum current electrode separation (AB/2) 100 m.

The data acquired were interpreted and analysed using lPl2win and Surfer 12 soft programs. The analysis of the interpreted data allowed the delineation of three (3) groundwater potential zones in the study area namely: good, moderate and poor groundwater potential zones.

5.2 Conclusion

The VES interpretation of Ungwan Mai Zanko and its environs shows that the area generally has good potential for groundwater.

The VES interpretation showed that the subsurface in the area consist of a maximum of five (5) layers with three (3) case scenarios including three (3) layer cases, four (4) layer cases and five (5) layer cases. The four layer case however, dominates. The layers include the top layer, the lateritic layer, the weathered layer, fractured layer and the fresh basement. The weathered layer represent the best potential for groundwater, however the fractured layer with good thickness could also represent a good groundwater bearing formation.

The area is made up of six (6) curve types including H, HA, QH, KH, QHA and KQH type curves with the dominant curve type being the QH with 13, representing 43.33% of the total curve types followed by the KH type with nine (9) representing 30% of the total curve types.

The geoelectric parameters (Resistivity and thickness) derived from the VES interpretations were used to generate contour maps of top layer resistivity, true aquifer resistivity, true aquifer thickness and overburden thickness (depth to basement). The four maps show good correlation and indicate that the central part of the area, with low top layer resistivity, low true aquifer resistivity, higher true aquifer thickness and higher overburden thickness represent the best groundwater potential zone.

The KU type curves dominate the good groundwater potential zone along with KQH and H type curves. This quite agree with the work of Ornosuyi (2010); 1-lur & Afa (2002) and Keller & Freschneit (1966) who stated that the H and KH type curves are often associated with good groundwater bearing zones in the Basement Complex terrains.

2.3 Recommendations

Based on the above findings and conclusions, it is thereby recommended that VES 10, 11, 14, 15, 16, 20 and 22 which fall within the good groundwater potential zone should be considered for exploitation in any future groundwater supply project in the area because they represent the best prospects for groundwater yield. However, the VES points within the moderate groundwater potential zone can as well be exploited especially if the intended water supply scheme will be used for domestic purposes.

REFERENCES

Abdel Aal, G.Z., Atekwana, E.A., Slater, L.D., Atekwana, E.A., (2004). Effects of microbial processes on electrolytic and interfacial electrical properties of unconsolidated sediments: Geophysycal Research Letters, 31, 1-4.

Abimbola, A. F., Akadang, J.A., Akande, S .0. and Olatunji, A .S. (2002). Environmental impact assessment of the heavy metals associated with Pb-Zn mineralization in Abakaliki area, south-eastern Nigeria. Extended Abstracts of the Quadrenmial IAGOD symposium and Geo-congress, Namibia 1-2.

Adegoke, 0 .S. (1969). Eocene stratigraphy of south-western Nigeria. Bull. Bur .Rosh. Geol. Mm Mem 69; 23-24.

Adegoke, 0. S (1970). Macrofauna of the Ewekoro formation (Paleocene) off south-western Nigeria (in)African Geology Dessuvagie, T.F.J. and Whiteman, A. J, Eds Univ Of Ibadan press, Nigeria 269-276.

Adegoke, 0. S. (1970). Type section Ewekoro formation (Paleocene) of western Nigeria,

th .

biostratigraphy and microfacies .4 African Micropal.CoIl Abidjan (1970), 3 7-39.

Adegoke, 0. S., Dessuvagie, T. F. J., Kogbe, C. A. and Ogbe, F.A. (1970). Type section Ewkoro formation (Paleocene) of south-western Nigeria bio-stratigraphy and macrofacies. 4th African Micropal.Coll Abidjan (1970), 37-39.

Agagu, O.K. (1985). A Geological guide to bituminous sediments in South Western Nigeria unpub report Department of Geology, University of Ibadan. 125.

Aguilar.(2003). Oil pollution detection using resistivity sounding, GeofIsica Internacional, Vol.42, pp. 6 13-622.

Aleixei, A.B. (2002). IPl2win(MT. Automated and Interactive semi-automated Interpretation of Magnetotelluric Sounding Data using Amplitude and/or phase curves. geoscanM limited.

Ameloko, A.A. & Rotimi, 0.J. (2010). 2D electrical imaging and its application in Groundwater exploration in parts of Kubanni River Basin, Zaria, Nigeria. World Rural Observations, 2 (2), 72-82.

Atakpo E. A. (2013). Resistivity Imaging of Crude Oil Spill jn Ogulaha Coastal Community, Atakpo, E,A. and Ayolabi, E.A.(2008). Evaluation of Aquifer Vulnerability and the

Protective Capacity in some Oil Producing Communities of Western Niger Delta. Environmentalist Springer. DO! 10.1007/s 10669-008-9193-3.

Bailey, N. J. L., Krouse, H. R., Evans C. R., and Rogers M. A. (1973). Alteration of Crude Oil by Waters and Bacteria - Evidence from Geochemical and Isotope Studies. American Association of Petroleum Geologist Bulletin. 57 (7): 1276 — 1290.

Batayneh, A.T.(2005). 2D Electrical imaging of an LNAPL contamination, Al Amiriyya fuel station, Jordan: Journal of Applied Sciences, 5, 52-59.

Bauman, P., Sallomy, J., Wong, T. and Hardisty, P. (1993). Geophysical data processing techniques as related to groundwater contamination studies. Proc. Symposium. Application of Geophysics to Engineering and Environmental Problems. EEGS, San Diego, CA. Pp. 167-180.

Bergreen, W. A. (1960). Paleocene bio-stratigraphy and planktonic foraminifera of Nigeria West Africa proc.2lSt Intern Geol Cong Copenhagen sec 6 pp 4 1-45.

Billsman, H.G. (1976). Offshore stratigraphy and Palaeontology of Dahomey Embayment, th

Proceedings 7 Afro Macropal College, Ile-Ife, (in Press).

Burutu L. G. A., Delta state, Nigeria. International Journal of Research and Reviews in Applied Sciences (IJRRAS). 15 (1): 97-10 1.

Busseli, G., Barber, C., Davis, G. B. and Salama, R. B. (1990). Detection of groundwater contamination near waste disposal sites with transient electromagnetic and electrical methods. Geotechnical and Environmental Geophysics, Society Exploration Geophysics, Tulsa, OK, pp. 27-39.

Daniel J. J., Roberts R. and Vendl H. (1995). Ground Penetrating Radar for the detection of liquid contaminants. Journal of Applied Geophysics. 33: 195-207.

De la Vega, M., Osella, A., Lascano, E., (2003). Joint inversion of Wenner and dipole-dipole data to study a gasoline-contaminated soil: Journal of Applied Geophysics, 54, 97-

109.

Delgado-Rodriguez 0, Shevnin .V, J.Ochoa-Valdes and A. Ryjov.(2006). Geophysical characterization of a site with hydrocarbon contamination caused by pipeline leakage,Geofisica Internacional, Vol.45, pp.63-72.

Dey, A., & Morrison, H. (1979). Resistivity modeling for arbitrarily shaped threedimensional structures. Geophysics, 44(4), 753-780.

Ernstson K, and Kirsch R (2006). Geoelectrical methods, basic principles. — In Kirsch R (ed):

Groundwater Geophysics: A Tool for Hydrology, 85—108. Springer.

Ernstson, K. and Kirsch, R. (2006). Geoelectrical methods. in: R. Kirsch (ed) Groundwater geophysics: A tool for hydrogeology. Springer, Berlin. 493p

Estella A. Atekwana and Eliot A. Atekwana(2009).Geophysical signature of microbial activity at hydrocarbon contaminated sites: A review, Surv Geophys, DOl

10.1007/si 0712-009-9089-8.

Estella A. Atekwana et al (2004a). Evidence for microbial enhanced electrical conductivity in hydrocarbon contaminated sed iment,GEOPHI SICAL RESEARCH LETT'ERS,Vol.31, pp. L23591.

Estella A. Atekwana et al (2004b).In-situ apparent conductivity measurements and microbial population distribution at a hydrocarboncontaminated site, GEOPHYSICS, Vol.69, NO.1, PP. 56-63.

Estella A. Atekwana, D. D. Werkema and Eliot A. Atekwana(2006). Biogeophysics: The effects of microbial processes on Geophysical properties of the shallow subsurfaces, Applied Hydrogeophysics, pp. 161-193.

Estella A. Atekwana, W. A. Sauck and D. D.Werkema Jr(2000).Investigation of geoelectrical signature at a hydrocarbon contaminated Site, Jumal of Applied Geophysics, Vol.44,pp. 167-181.

Fayose, E. A. (1970). Stratigraphical Paleontology of Afowo 1 well SW Nigeria Jour. Mm. Geol. Nigeria. 5, (1).

Godio, A., Naldi, M.(2003). Two-dimensional electrical imaging for detection of hydrocarbon contaminants: Near Surface Geophysics, 1, 131-137.

Henriet, J.P. (1976). Direct Application of the Dar-Zarrouk Parameters in Groundwater Surveys. Groundwater Prospecting, 24 (2): 344 — 353

Hernández-Márquez, J.O., RodrIguez-Villuendas, A., (2008). Aplicación de métodos geoeléctricos para el diagnóstico de un sitio urbano contaminado por hidrocarburos:

Mexico, D.F., Mexico, Facultad de IngenierIa, Universidad Nacional Autónoma de Mexico, tesis de licenciatura, 149 p.

Jatau, B.S., Patrick, N.O., Baba, A. & Fadele, S.l. (2013). The use of Vertical Electrical Sounding (VES) for subsurface geophysical investigation around Bomo area, Kaduna State, Nigeria. IOSR Journal of Engineering, 3:10-15.

Jones, H. A. and Hockey, R. D. (1964). The Geology of parts of Southwestern Nigeria. Geological Survey of Nigeria. Bull 31; 56 — 71.

Keller, G.V. & Frischneit, F.C. (1966). Electrical methods in geophysical prospecting. Pergamon press, Oxford, New York. 254.

Kirsch, R. (2007). Petrophysical properties of permeable and low-permeable rocks. In: R. Kirsch (ed) Groundwater geophysics: A toolfor hydrogeology. Springer, Berlin. 493p

Lenkey, L., Hamori, Z. & Mihaiffy, p. (2005). Investigating the hydrogeology of a water supply area using direct current vertical electrical soundings. Geophysics, 70(4),

1-19.

Loke, M. H. (1999). Electrical imaging surveys for environmental and engineering studies. A practical guide to 2-D and 3-D surveys Copyright (1997, 1999, 2000) Available online at www.geoelectrical.com.

Loke, M. H. (2011). Electrical resistivity surveys and data interpretation. In: Gupta HK ed. Encyclopedia of Solid Earth Geophysics. 2nd ed. s.l.: Springer, pp.276—283.

Loke, M. H. (2011). Tutorial : 2-D and 3-D electrical imaging surveys. [Online] Available at:

www.geoelectrical.com [Accessed 15 June 2012].

Loke, M. H. (2013). Tutorial: 2D and 3D electrical imaging surveys. Geotomo Software,Malaysia.

Loke, M.1-l. (1999). Time-lapse resistivity imaging inversion. Proceedings of the 5th Meeting of the Environmental and Engineering Geophysical Society European Section, Eml.

Loke, M.H., Acworth, 1., and Dahlin, T. (2003). A comparison of smooth and blocky inversion methods in 2D electrical imaging surveys. Exploration Geophysics 34: 182-

187.

Maillet, R. (1974). The Fundamental Equations of Electrical Prospecting. Geophysics, 12 (4):

529 - 556

Milenko, B. and Mirjana, S.B. (2014). Geo electricnl Signature of Long Term HydrocarbonContamination in Serbia. International Journal of Science and Research

(IJSR), 3(5): 2319—7064.

Modin,l.N, Shevnin,V. A., Bobatchev, A. A., Bolshakov, D.K., Leonov, D.A. and Vladov,

M. L. (1997). Investigations of Oil Contamination with Electrical Prospecting Methods. Proceedings of the 3rd EEGS-ES Meeting, Aarhus, Denmark. Pp 267-270.

Moreno, M.A. and Galván, C.A. (2013). Use of Electrical Resistivity Tomography in the Study of Soil Pollution caused by Hydrocarbons: Case Study in Puebla (Mexico). Boletin De La Sociedad Geologica Mexicana, 65 (2): 419 - 426

NESREA, (2009). Regulations. National Environmental Standards and Regulation Enforcement Agency (NESREA), 96 (65): The Federal Government Printer, Abuja, Nigeria.

Newmark, R.L., Ames. R.D., Hudson. G.B., Leif, R., Chirappa, M., Carrigan, C., Nitao, J.J., Elsholz, A., Eaker, C., (1999). An integrated approach to monitoring a field test of in

situ contaminant destruction: Proceedings for SAGEEP, Oakland, California, U.S.A.,

527-540.

Nweke, O.C. and Sander, W.H. (2009). Modern Environmental Health Hazards: A Public Health Issue of increasing Significance in Africa. Environmental J-lealth Perspective,

117(6): 863—870.

Ogbe, F. A .G. (1970). Stratigraphy of strata exposed in Ewekoro Quarry Western Nigeria African geology Dessuvagie T F J and Whiteman A J (lEds) Univ of Ibadan Press, Nigeria 305-324.

Oladapo, M.1., Mohammed, M.Z., Adeoye, 0.0. and Adetola, B.A. (2004). Geoelectricai investigation of the Ondo State Housing Corporation Estate, Ijapo Akure, Southwestern Nigeria. Journal of Mining and Geology, 40 (1): 41 — 48.

Omatshola, M. E. and Adegoke, 0. S. (1981). Tectonic evolution of the Dahomey basin.Journai of Mining Geol. 54; 65- 87

Ozumba C. 1., Ozumba M. B., Obobaifo C. E. (1999). Striking a balance between oil exploration and protecting the environment. NAPE Bulletin. 14 (2): 130-135.

Ramakrishnalah, C.R, Sadas hivalah C. and Ranganna Q, (2009). Assessment of water quality index for the groundwater in Tumkur Taluk , Karnataka State. India, EJournal of Chemistry, 6(2): 523-530.

Reyment, R. A. (1957). Notes on some Globigerinidae Globatruncanidae and Globorotaliidae from the Upper Cretaceous and Lower Tertiary of western Nigeria record Geol Surv Nigeria 68-86.

Reyment, K. A. (1963). Studies of Nigerian Upper Cretaceous and Lower Tertiary Ostracoda Stockh contrib. Geol 7,238,23.

Reyment, R. A. (1964). Review of the Nigerian Cretaceous and Cenozoic stratigraphy Jour Mm Geol 2 (2); 6 1-80.

Reyment, R. A. (1965). Aspect of Geology of Nigeria, University Press. 133; 18.

Reyment, R. A. (I 965a). Quantitative Paleoecologic analysis of Ewekoro and Oshosun Formations of western region ofNigeria Geol Forem Stockh Forbanail 86:248-256.

Reyment, R. A. (1 966a). Excursion to Ewekoro area western region of Nigeria Jour. MinGeol,2(1); 11.

Reyment, R. A. (1966b). Brief review of the stratigraphic sequences of West Africa Angola Senegal proc 2' African Micropal coil Ibadan 1965 ;162-175.

Reynolds, J. M. (201 1). An introduction to applied and environmental geophysics:

John Wiley & Sons.

Robinson, E. S. (1988). Basic Exploration Geophysics, John wiley & Sons. Inc.

Russ, W. (1924). The phosphate deposit of Abeokuta province Geol. Surv Nigeria bull. 38;46.

Sauck, W.A., Atekwana, E. A., and Nash, M. S. (1998). High conductivities associated with an LNAPL plume imaged by integrated geophysical techniques. JEEG, 2, 203-2 12.

Shevnin .V, 0. Delgado-Rodriguez, A. Mousatov, E. Nakamura-Labastida and A.Mejia

APPENDICES

APPENDIX (A)

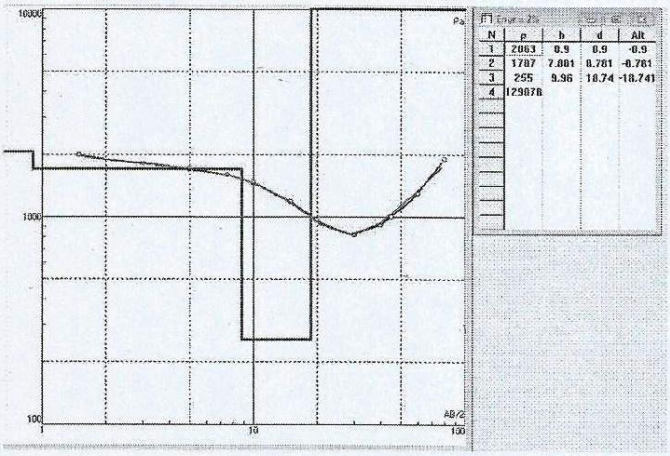


Figure 1: VES 1

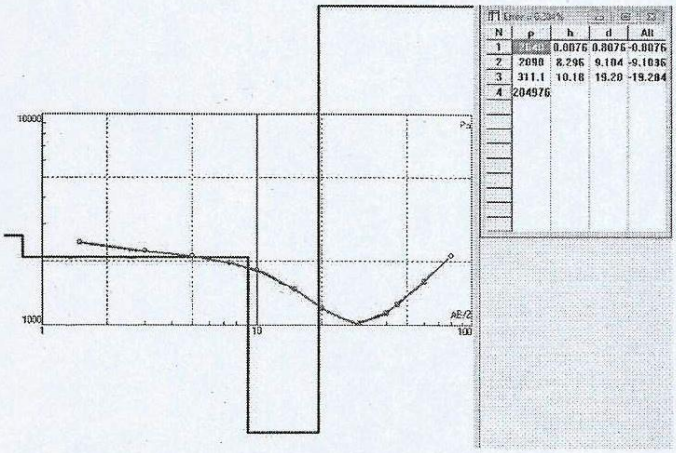


Figure 2: VES 2

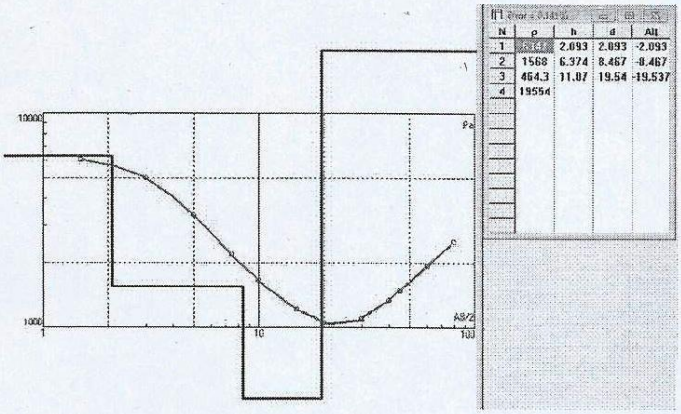
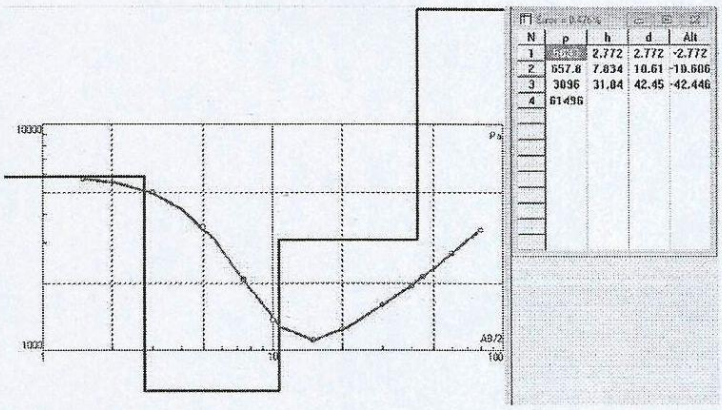
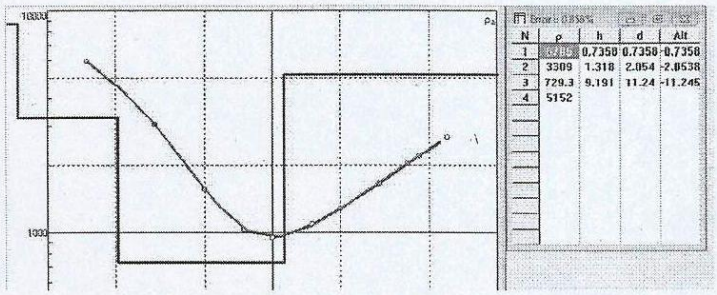


Figure 3: VES 3



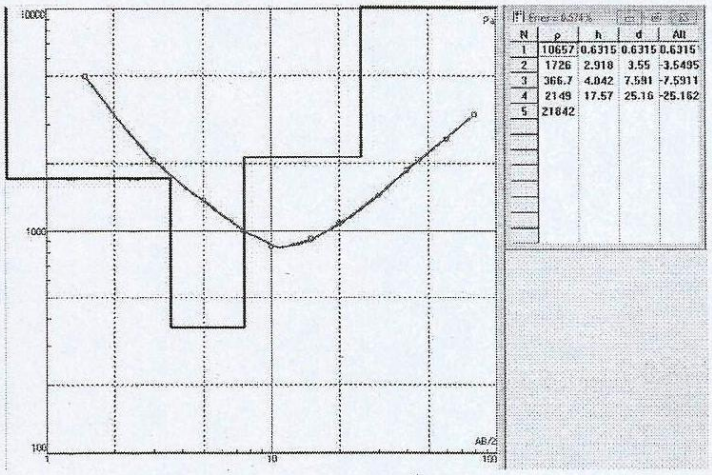
N	ρ	h	d	Alt
1	657.8	2.772	2.772	-2.772
2	657.8	7.834	10.61	-10.606
3	3096	31.84	42.45	-42.446
4	61496			

Figure 4: VES 4



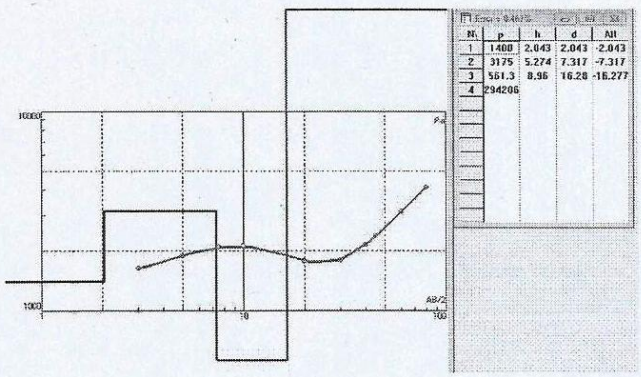
N	ρ	h	d	Alt
1	3309	0.7358	0.7358	-0.7358
2	3309	1.318	2.054	-2.0538
3	729.3	9.191	11.24	-11.245
4	5152			

Figure 5: VES 5



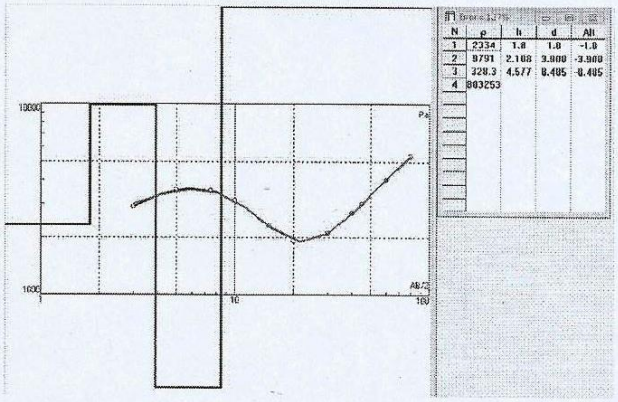
N	ρ	h	d	Alt
1	10657	0.6315	0.6315	0.6315
2	1726	2.918	3.55	-3.5495
3	366.7	4.042	7.591	-7.5911
4	2149	17.57	25.16	-25.162
5	21842			

Figure 6: VES 6



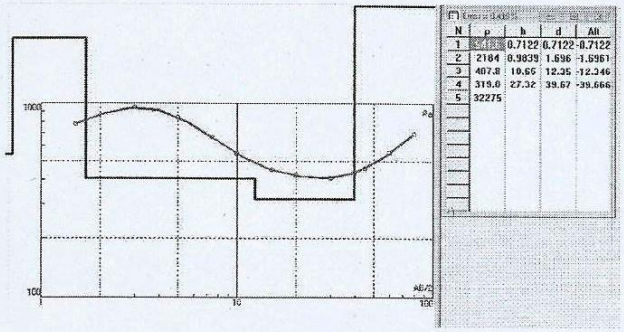
N	ρ	h	d	Alt
1	1400	2.043	2.043	-2.043
2	3175	5.274	7.317	-7.317
3	561.3	8.96	16.28	-16.277
4	294206			

Figure 7: VES 7



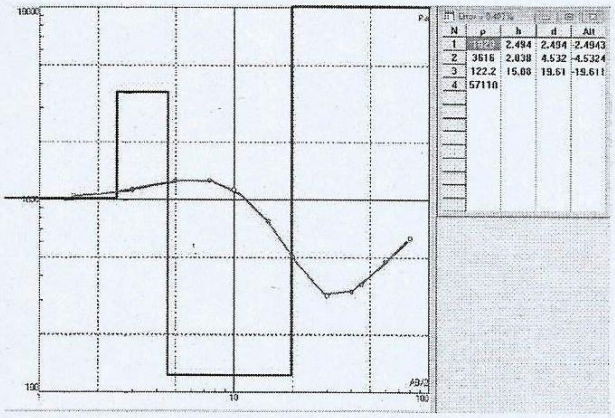
N	ρ	h	d	Alt
1	2334	1.8	1.8	-1.8
2	9791	2.108	3.908	-3.908
3	328.3	4.577	8.485	-8.485
4	803253			

Figure 8: VES 8



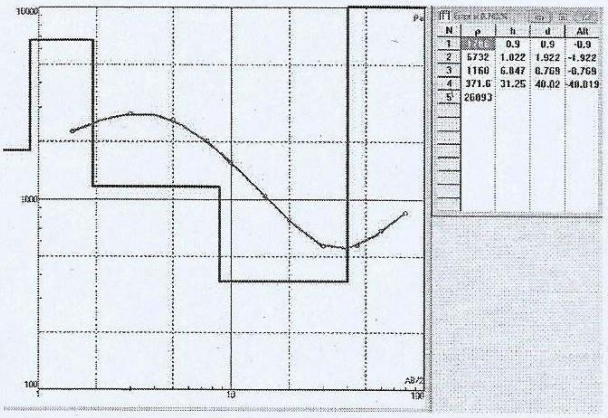
N	ρ	h	d	Alt
1	[illegible]	0.7122	0.7122	-0.7122
2	2184	0.9839	1.696	-1.6961
3	407.8	10.65	12.35	-12.346
4	319.0	27.32	39.67	-39.666
5	32275			

Figure 9: VES 9



N	ρ	h	d	Alt
1	[illegible]	2.494	2.494	-2.4943
2	3616	2.038	4.532	-4.5324
3	122.2	15.08	19.61	-19.611
4	57110			

Figure 10: VES 10



N	ρ	h	d	Alt
1	[illegible]	0.9	0.9	-0.9
2	5732	1.022	1.922	-1.922
3	1160	6.847	8.769	-8.769
4	371.6	31.25	40.02	-40.019
5	26093			

Figure 11: VES 11

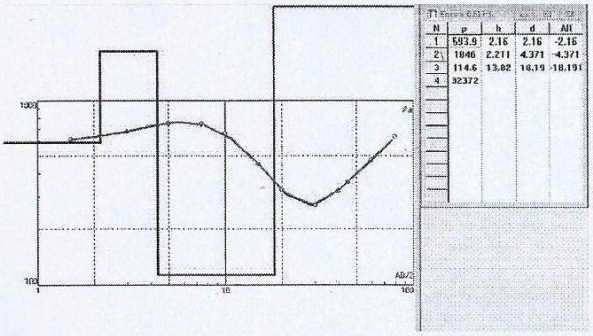


Figure 12: VES 12

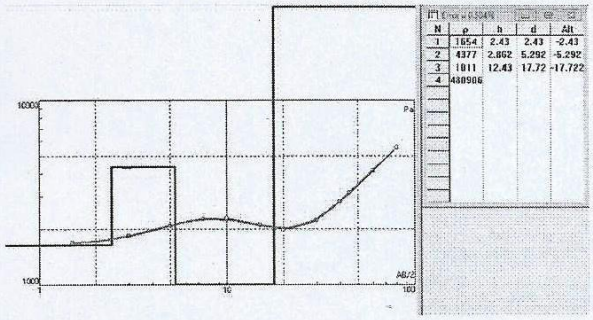


Figure 13: VES 13

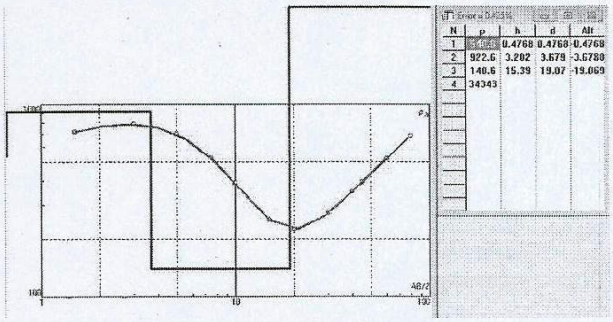


Figure 14: VES 14

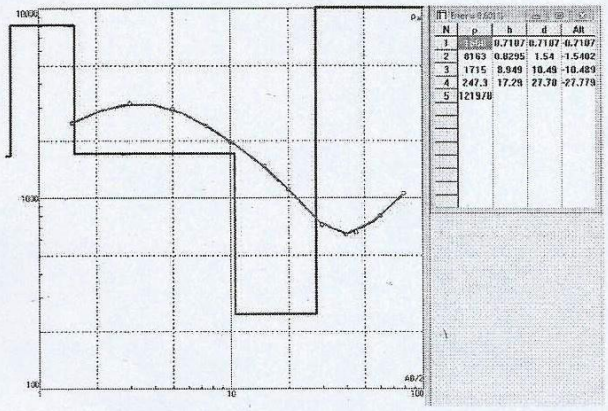
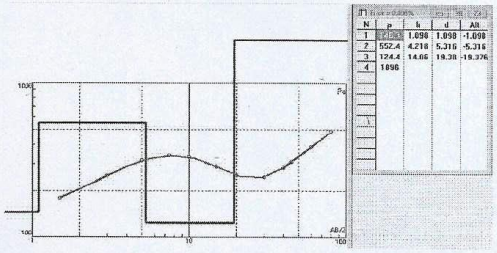
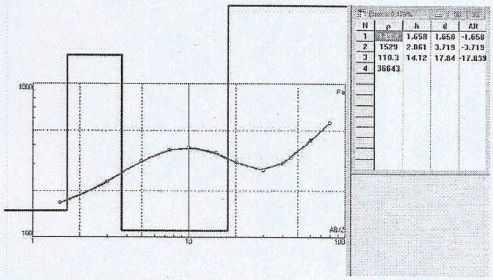


Figure 15: VES 15



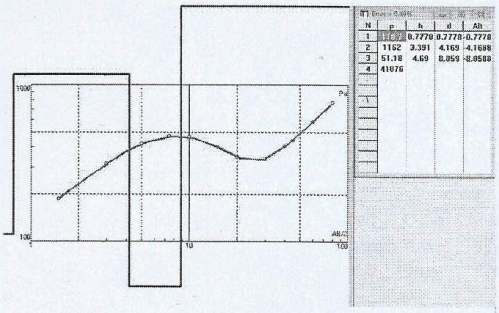
N	ρ	h	d	Δh
1	2182	1.098	1.098	-1.098
2	552.4	4.218	5.316	-5.316
3	124.4	14.06	19.38	-19.376
4	1896			

Figure 16: VES 16



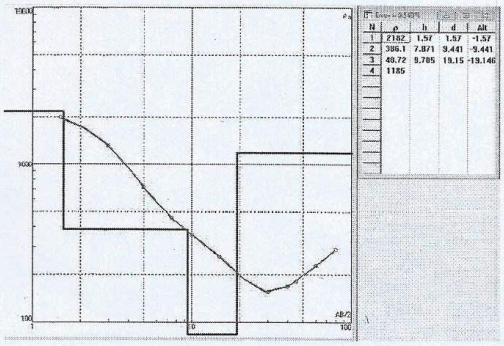
N	ρ	h	d	Δh
1	2182	1.658	1.658	-1.658
2	1529	2.061	3.719	-3.719
3	110.3	14.12	17.84	-17.859
4	38643			

Figure 17: VES 17



N	ρ	h	d	Δh
1	2182	0.7778	0.7778	-0.7778
2	1162	3.391	4.169	-4.1688
3	51.18	4.69	8.859	-8.8588
4	41076			

Figure 18: VES 18



N	ρ	h	d	Δh
1	2182	1.57	1.57	-1.57
2	386.1	7.871	9.441	-9.441
3	40.72	9.705	19.15	-19.146
4	1185			

Figure 19: VES 19

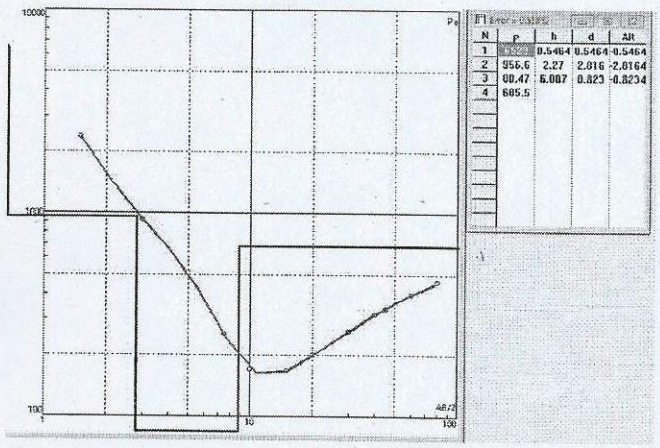


Figure 20: VES 20

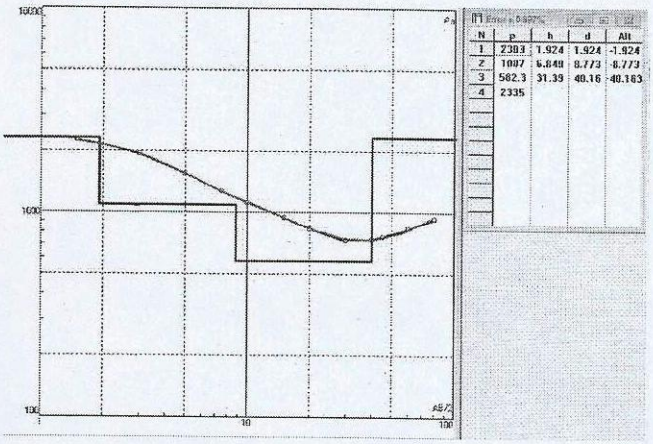


Figure 21: VES 21

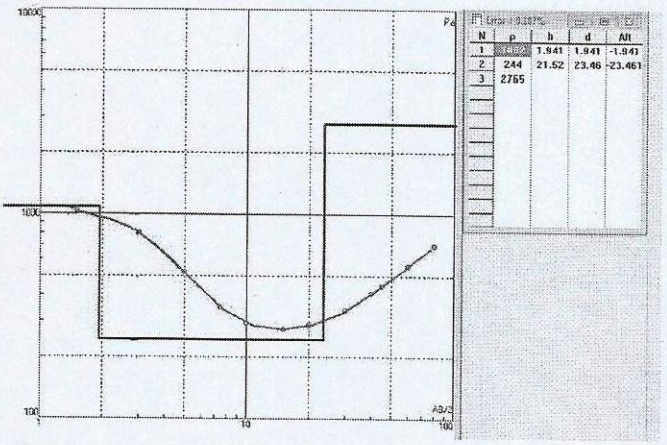


Figure 22: VES 22

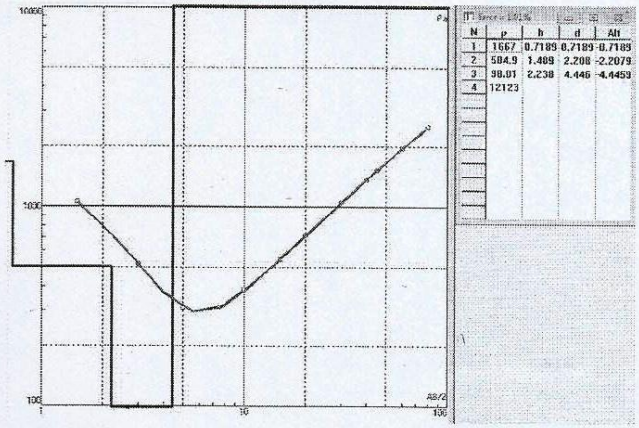


Figure 23: VES 23

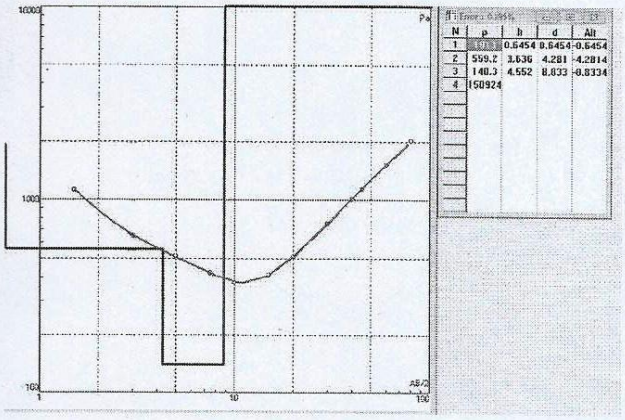


Figure 24: VES 24

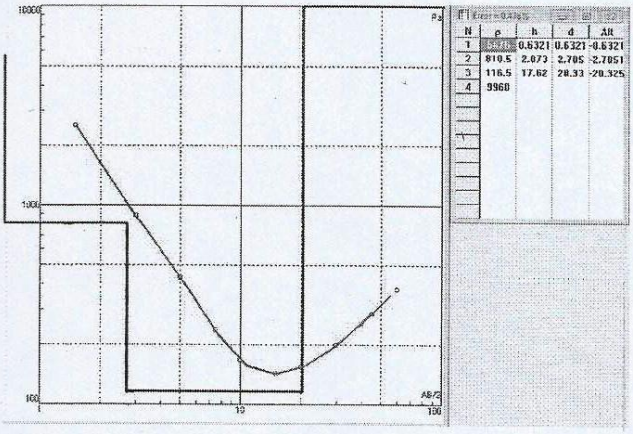


Figure 25: VES 25

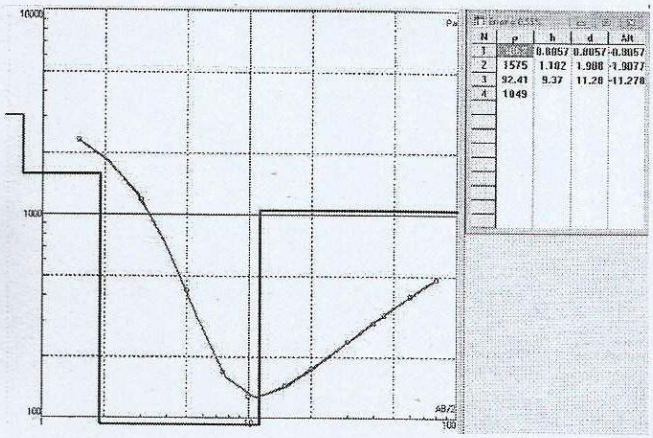


Figure 26: VES 26

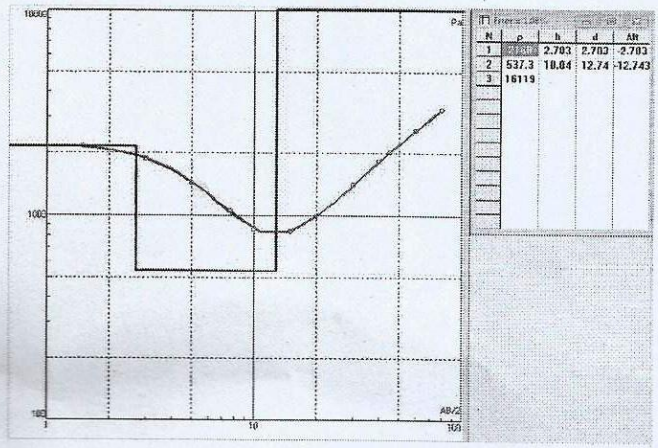


Figure 27: VES 27

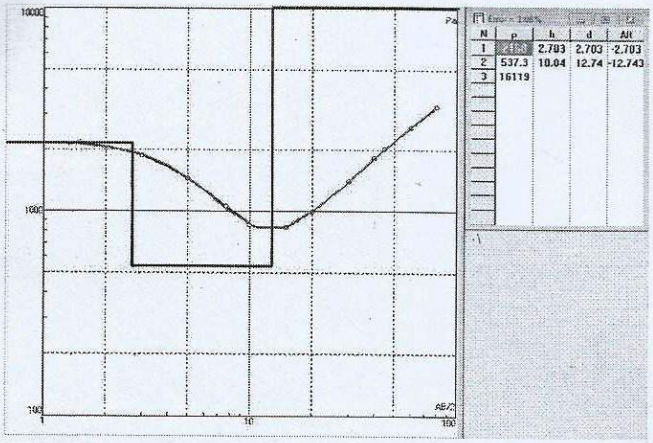


Figure 28: VES 28

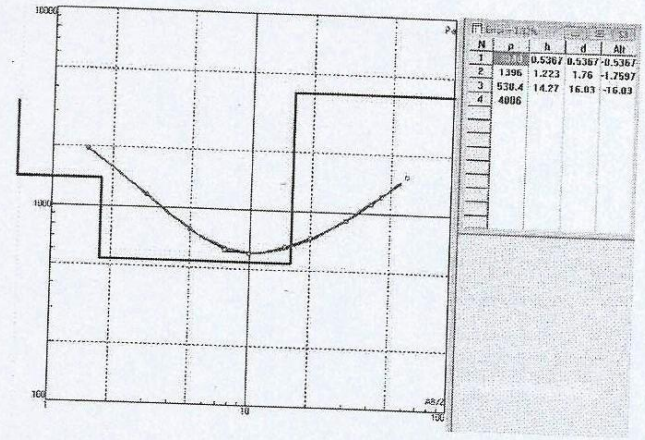


Figure 29: VES 29

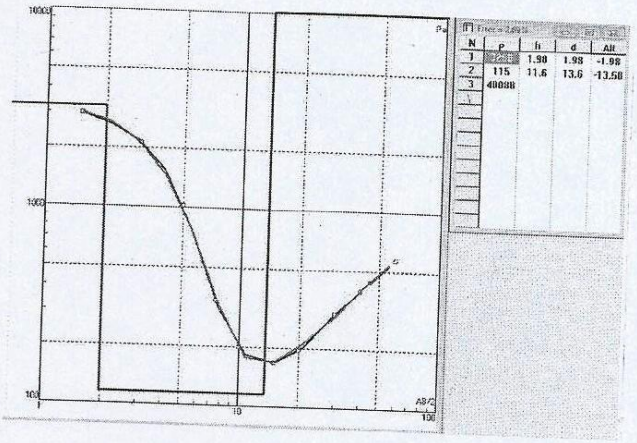


Figure 30: VES 30